Journal of Applied Biology & Biotechnology Vol. 10(6), pp. 60-80, Nov-Dec, 2022
Available online at http://www.jabonline.in
DOI: 10.7324/JABB.2022.100607

Identification of phytocompounds from *Paris polyphylla* Smith as potential inhibitors against two breast cancer receptors (ERα and EGFR tyrosine kinase) through chromatographic and *In silico* approaches

Debmalya Das Gupta[1], Saurov Mahanta[2], Sasti Gopal Das[3], Sanjib Kumar Das[1], Dipayan Paul[1], Hui Tag[4], Pallabi Kalita Hui[1]*

[1] Department of Biotechnology, National Institute of Technology Arunachal Pradesh, Jote – 791113, Papum Pare, Arunachal Pradesh, India.
[2]National Institute of Electronics and Information Technology, Guwahati -781008, Assam, India.
[3]Bioinformatics Center, Vidyasagar University, Midnapore-721102, West Bengal, India.
[4]Pharmacognosy and Phytochemistry Research Laboratory, Department of Botany, Rajiv Gandhi University, Rono Hills-791112, Doimukh, Arunachal Pradesh, India.

ARTICLE INFO

Article history:
Received on: April 27, 2022
Accepted on: August 21, 2022
Available online: September 20, 2022

Key words:
Breast cancer,
Paris polyphylla,
Steroidal saponins,
Molecular docking,
Binding affinity,
Molecular simulation.

ABSTRACT

In the current decade, the potential side effects caused by synthetic kinase domain inhibitors have paved the way for developing an alternative anti-breast cancer drug from botanical sources. Estrogen receptor-α (ERα) and epidermal growth factor receptor (EGFR) tyrosine kinase receptors play a key role in the activation of genomic and non-genomic related pathways of breast cancer progression. *Paris polyphylla* Smith (Melanthiaceae) is a rich source of steroidal saponins reported as an anti-breast cancer agent used among the local communities of Asian countries. In the present study, a total of 116 phytocompounds were characterized and identified from *P. polyphylla* rhizomes using gas chromatography–mass spectrometry and liquid chromatography–mass spectrometry tools. They were subjected to virtual screening, molecular docking, and molecular simulation analysis with these two breast cancer receptors. Among them, only three steroidal saponins, namely, diosgenin, pennogenin, and 7-ketodiosgenin acetate binding affinity with target receptors were on the higher side when compared with natural ligands. The highest affinity for the receptors ERα and EGFR tyrosine kinase was shown by 7-ketodiosgenin acetate with docking scores of −10.4 Kcal/mol and −11.2 Kcal/mol, respectively, followed by diosgenin and pennogenin. LigPlot$^+$ analysis revealed that the selected three steroidal saponins utilized a combination of hydrogen bonding and hydrophobic interactions to align themselves more efficiently in the ligand-binding pocket of the target receptors. Molecular simulation analysis revealed a stable interaction between the phytocompounds and the target receptors. Lipinski's rule confirmed pennogenin as the best phytocompound that could be used as a potential inhibitor against the two target breast cancer receptors (ERα and EGFR tyrosine kinase).

1. INTRODUCTION

During the past several decades, the basic information on cancer biology has provided a ray of hope for developing gene-targeted cancer therapy. However, cancer continues to be one of the top killers of humankind [1]. Various factors aid in the progression of cancer, namely, transformation, survival, proliferation, invasion, angiogenesis, and metastasis. Among the several cancers types reported, breast cancer is one of the top killers of women globally, while in 2019, the number of females with breast cancer residing in the United States was more than 3.8 million, and the mortality of patients due to breast cancer is estimated to be around 15% [2,3]. The majority of breast cancer deaths are due to metastasis of the disease to the lungs, bone, and brain. However, death due to breast cancer has been reported more in the developing countries, especially among Black women of the African region. Several factors, including late diagnosis, and high incidence of obesity, coupled with unfavorable tumor properties, have been cited as a significant reason for increased mortality among women with breast cancer [2]. Most breast cancer (approx. 70%) cases reported are hormone receptive [4]. Being a heterogeneous disease, it expresses several hormone receptors, namely, estrogen receptor (ER), progesterone receptor (PR), and human epidermal growth factor receptor 2 (HER2). Estrogen signaling follows both the genomic and non-genomic pathways. In the genomic pathway, ERs such as ERα and ERβ play an essential role in activating cancer-related pathways. In hormone-dependent cancer types such as breast

*Corresponding Author:
Pallabi Kalita Hui, Department of Biotechnology, National Institute of Technology Arunachal Pradesh, Yupia, Papum Pare, Arunachal Pradesh, India.
E-mail: pallabi2008rgu @ gmail.com

cancer, endometrial cancer, and ovarian cancer, ERα promotes cancer formation [5]. Natural estrogen, namely, 17 β-estradiol, upregulates cellular Myc and cyclinD1 expression, stimulating the migration of epithelial cells present in mammary glands from the G1 phase to the S phase [6]. Moreover, an active ER pathway automatically increases the expression of progesterone in breast cancer cells since it is the end product of ER stimulation. Hence, blocking the active site of the ER that binds to this natural ligand could prevent the binding of the natural estrogen, thereby blocking subsequent steps for cancer progression [7].

However, estrogen signaling can also be mediated by a non-genomic pathway. This involves secondary messengers and interaction with membrane receptors such as EGFR tyrosine kinase [8]. Phosphorylation of EGFR initiates further signal transduction events such as stimulation of Src, phosphatidylinositol-3-kinase, serine/threonine-protein kinase (Akt), and mitogen-activated protein kinase, leading to cancer formation [9]. Tyrosine kinase inhibitor (TKI) drugs such as erlotinib and gefitinib bind to EGFR tyrosine kinase reversibly and block further signaling events and, hence, be able to stop the growth of cancer cells. Since breast cancer results from the dysregulation of multiple genes, targeting only a particular pathway may render the drug less potent [10]. Therefore, targeting multiple inflammatory pathways using phytocompounds from traditional medicinal plants could provide new opportunities and insights for cancer prevention and treatment. They are readily available in nature, have low cost, and potential to modulate multiple cell signaling pathways and potential check tumor development [11].

The genus *Paris* belonging to the family Melanthiaceae has 36 species and 10 varieties worldwide. However, the majority of the species are reported from Eurasian plains, Eastern Himalayas, and the parts of Asia, particularly in South Central and South-East regions of China, India, Nepal, Bangladesh, Bhutan, Myanmar, Laos, Thailand, Tibet, and Vietnam [12,13]. It is also found distributed inside the forest floor of moist subtropical and temperate regions of Kameng, Subansiri, Kurung Kumey, Siang, Lohit, Tirap, and Changlang districts (ca 1800–3000 m) of the Arunachal Himalayan Region (AHR) of India [14,15]. The rhizome is reported to cure several ailments such as cancer, Alzheimer's, abnormal uterine bleeding, and leishmaniasis [16]. The local tribal communities of the Eastern Himalayan region of India use the rhizome as an antidote for snake and insect poison [17]. The steroidal saponins are the major class of compounds reported from *Paris polyphylla* rhizomes and also comprise triterpenoid saponins [18,19], while steroidal saponins such as dioscin, polyphyllin D, and balanitin 7 are reported as bioactive phytocompounds from the rhizome of *P. polyphylla* Smith [20]. Recent phytochemical studies on *P. polyphylla* from Eastern Himalaya have confirmed the diosgenin and other steroidal saponins, namely, pennogenin and 7-Ketodiosgenin acetate as major bioactive phytoconstituents [19]. However, molecular docking studies of individual phytoconstituents (steroidal saponins) of *P. polyphylla* effective against specific breast cancer receptors are not reported to date.

The purpose of this study is to identify bioactive steroidal saponins from *P. polyphylla* rhizome as effective inhibitors against breast cancer receptors, namely, ERα EGFR tyrosine kinase [Figure 1] through the *in silico* approach using AutoDock 4.1 program suite of MGL Tools 1.5.4 software. AutoDock software is widely used as a computational tool, and it is simple, cost free, more realistic in energy prediction, and uses wider conformational space in the protein. It has the edge over other methods having low conformational space constrained by several factors, namely, rigidity in receptor and bond angles and simplified scoring function based on free energies of binding [21].

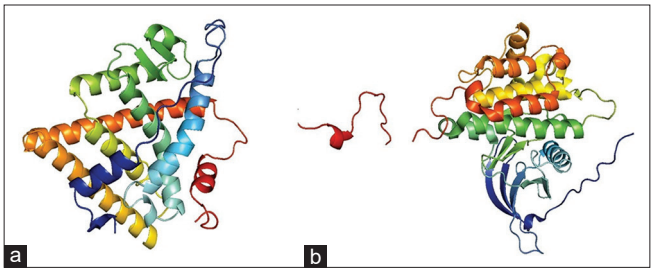

Figure 1: (a) Estrogen receptor α (PDB ID: 3ERT) and (b) epidermal growth factor receptor tyrosine kinase (PDB ID: 1M17).

2. MATERIALS AND METHODS

2.1. Sample Collection and Preparation of Ethanolic Extract of *P. Polyphylla* Rhizome (EEPPR) for Liquid Chromatography–Mass Spectrometry (LC–MS) Characterization

P. polyphylla rhizomes were collected from the subtropical forest area of Godak (28°21'50.38"N and 92°80'36.77"E) in Kamle district of Arunachal Pradesh (Eastern Himalayan Region of India). The voucher specimen No. 06/DD/HT/2019 dated May 11, 2019 of *P. polyphylla* was prepared and authenticated at BSI ASSAM Herbarium, Shillong, and the accepted name was verified at www.plantsoftheworldonline.org (POWO) and deposited to Herbarium of Arunachal University, Department of Botany, Rajiv Gandhi University, Rono Hills, Doimukh-791112, Arunachal Pradesh, for future reference [22]. Clean and oven-dried (35–40°C) *P. polyphylla* rhizomes were sliced and subsequently powdered. It was followed by soaking into 70% ethanol (1:10 ratio for sample: solvent) for 24 h without any heat with intermittent shaking using an orbital shaker (Cole-Parmer Model Stuart SSL1). The samples were then filtered (Whatman No. 1 filter paper) and were concentrated at a vacuum pressure of 200 Mpa, temperature 45–50°C in a rotary vacuum evaporator (IKA Model No. GS90A24, Germany). The concentrated crude extract (10% w/v) – EEPPR obtained was stored in a freezer at 4°C keeping chemical degradation at bay and was further used for LC-MS characterization of the phytocompounds.

2.2. LC–MS Characterization of Phytocompounds

The LC–MS characterization of the EEPPR was performed in LC–MS (Thermo Scientific Plus with Dionex Ultimate 3000) using a C18 column having a diameter of 150 × 2.1 mm and particle size of 1.9 µ at room temperature. The sample volume injected was 10 µL, with the mobile phase being acetonitrile and 0.2% aqueous acetic acid v/v, respectively. Sample running time was set at 20 min with flow rate fixed at 0.6 mL/min. The diode-array detection detector was set at 280 nm to obtain the respective chromatograms generated. Triple quadruple mass spectrometer (Thermo Scientific) pre-equipped with ion sources electrospray ionization with mass range for full scans m/z 50–6000 was used. The m/z values of the resolved peaks obtained were compared with m/z values obtained from public databases such as MassBank [23], METLIN [24], and HMDB [25].

2.3. Selection and Preparation of Compounds Library from *P. polyphylla* as Ligands

A total of 79 phytocompounds were characterized and identified from EEPPR through LC–MS studies which were used as a compound library [Table 1]. We also consulted and selected a total of 37 phytochemicals (compound library) reported earlier [19] from

Table 1: Phytocompounds characterized and identified from EEPPR using LC–MS tool.

S. No.	Chemical name	PPM	Molecular mass (g/mol)
1.	2,5-Dimethoxycinnamic acid	3	208.21
2.	Kaempferol	3	286.24
3	2-Benzylsuccinic acid	3	208.21
4.	Sinapyl aldehyde	3	208.073
5.	6-Methoxymellein	3	208.21
6.	2-Benzylsuccinate	3	208.21
7.	5-[(3,4-Dihydroxyphenyl) methyl] oxolan-2-one	3	208.073
8.	Furapiole	3	208.21
9.	1-(2-Methoxy-3,4-methylenedioxyphenyl)-1-propanone	3	208.21
10.	4-Methyl-4-aza-5-pregnene-3,20-dione	8	329.5
11.	Butanedioic acid	4	118.09
12.	Gallic acid	5	170.12
13	Chlorogenic acid	5	354.31
14.	Sumatriptan	9	295.402
15.	4-(8, 9-Dihydro-8-methyl-7H-1, 3-dioxolo (4,5-H) (2,3) benzodiazepin-5-yl) benzenamine	2	295.34
16.	Tetrahydrothiophene-2-carboxylic acid	8	132.18
17.	3-methyl sulfolene	8	132.18
18.	3-Oxo-3-ureidopropanoate	7	145.09
19.	5-N-Methyloxaluric acid	7	146.1
20.	3-Hydroxy-3-methyl-glutaric acid	8	162.141
21.	Levoglucosan	8	162.141
22.	2-Hydroxyadipic acid	8	162.140
23.	3,3-diethoxy-1-propanol	8	148.2
24.	2S-Hydroxy-hexanedioic acid	8	162.14
25.	3-Hydroxymethyl-glutaric acid	8	162.141
26.	L-Rhamnono-1,4-lactone	8	162.14
27.	2-Dehydro-3-deoxy-L-rhamnonate	8	161.13
28.	2-Dehydro-3-deoxy-D-fuconate	8	162.14
29.	(R)-2-Ethylmalate	8	160.12
30.	5-Ureido-4-imidazole carboxylate	1	170.13
31.	Magnesium propionate	4	170.45
32.	1-Naphthoic acid	8	172.18
33.	Menadoine	8	172.18
34.	Dehydromatricaria ester	8	172.18
35.	Methyl (Z)-dec-2-en-4,6,8-triynoate	8	172.18
36.	1-Hydroxy-2-naphthaldehyde	8	172.18
37.	2-Naphthoic acid	8	172.18
38.	3Z-Undecene-5,7,10-triynoic acid	8	172.18
39.	4E-Undecene-6,8,10-triynoic acid	8	172.18
40.	L-Ascorbic acid	1	176.12
41.	2-Ketogulonolactone	1	194.14
42.	Glucuronolactone	1	176.12
43.	5-Dehydro-4-deoxy-D-glucuronate	1	175.12
44.	(4S)-4,6-Dihydroxy-2,5-dioxohexanoate	1	175.12
45.	2-Hydroxy-3-oxoadipate	1	176.12
46.	2-Hydroxydibenzofuran	8	184.19
47.	Dibenzo-p-dioxin	8	184.2

(Contd...)

Table 1: *(Continued)*

S. No.	Chemical name	PPM	Molecular mass (g/mol)
48.	4-Hydroxy-4-methyl-2-oxoglutaric acid	1	174.11
49.	D-Glucurono-6,2-lactone	1	176.12
50.	(4S,5S)-4,5-Dihydroxy-2,6-dioxohexanoate	1	176.032
51.	D-Galacturonolactone	1	176.12
52.	4-Hydroxybenzophenone	9	198.22
53.	Splitomicin	9	198.22
54.	3,4-Dihydroxyfluorene	9	198.22
55.	1,2-Dihydroxyfluorene	9	198.22
56.	Dehydrosafynol	9	198.22
57.	Capillarin	9	198.22
58.	2-Phenyl-3-(2-furyl) prop-2-enal	9	198.22
59.	4-Hydroxybenzophenone	9	198.22
60.	2-Phenyl-3-(2-furyl) prop-2-enal	9	198.22
61.	Porphobilinogen	6	226.22
62.	Carbidopa	6	226.23
63.	2-(2,4-Hexadiynylidene)-1,6-dioxaspiro[4.4]non-3-ene	1	220.23
64.	D-Erythro-Biopterin	1	237.21
65.	Orinapterin	1	237.21
66.	Dyspropterin	1	237.22
67.	Primapterin	1	237.22
68.	Sepiapterin	1	237.22
69.	N-Acetyl-D-glucosamine	5	221.21
70.	Glycolyl-D-mannosamine	5	237.21
71.	Deoxyeritadenine	5	237.22
72.	2-(7'-Methylthio) heptylmalic acid	4	276.35
73.	3-(7'-Methylthio) heptylmalic acid	4	276.35
74.	Purpuritenin B	5	292.3
75.	Purpuritenin A	5	292.3
76.	Coumatetralyl	5	292.33
77.	N-gamma-Glutamyl-S-propylcysteine	2	292.35
78.	(all-E)-1,7-bis (4-hydroxyphenyl)-1,4,6-heptatrien-3-one	5	292.334
79.	(2S,4S)-Monatin	8	292.29

P. polyphylla of the AHR characterized through gas chromatography–mass spectrometry profiling. Therefore, in the present docking study, 116 phytocompounds were selected from *P. polyphylla* rhizome. The chemical names, structure, and molecular weight were verified from Dr. Duke's Phytochemical and Ethnobotanical Database [26] PubChem and ChemSpider [27]. The 3D structures of the target phytochemicals were downloaded from various libraries (PubChem, zinc database, and ChemSpider). Finally, all the chemical structures were converted to PDB format with the help of PyMOLv0.99 [28].

2.4. Preparation of Receptor Proteins

The crystal 3D structure of ERα (PDB ID: 3ERT) and EGFR tyrosine kinase (PDB ID:1M17) was resolved by peer researchers through X-ray diffraction technique with a resolution of 1.90 Å and 2.60 Å, respectively [Figure 1]. The 3D structure of both the receptors was retrieved from the RCSB Protein Data Bank (www.rcsb.org/). The 3-D structure of the major active metabolite of tamoxifen, that is, afimoxifene docked with ERα (https://www.rcsb.org/structure/3ERT) and EGFR tyrosine kinase domain docked with 4-anilinoquinazoline inhibitor erlotinib (https://www.rcsb.org/structure/1M17), was also downloaded in required format from the RCSB PDB (https://www.rcsb.org/). After recording the active site information, the bounded natural ligands were removed from the complexes using UCSF Chimera and reconfirmed with a SWISS PDB viewer. The selected protein files were further optimized by eliminating the solvent water and unwanted residues. The result was visualized in BIOVIA Discovery Studio visualizer.

2.5. Molecular Docking Between Ligands and the Receptors

A computational docking experiment was conducted using the AutoDock 4.1 program suite using the MGL Tools 1.5.4 platform [29]. Different parameters such as polar hydrogens, Kollman charges, and atomic solvation charges were defined. The ligands, polar hydrogens, atomic charges, and flexible torsions were accordingly described for the ligands used in the docking. The corresponding docking parameter file was prepared using these parameters. The genetic algorithm was

selected for the docking simulations. The final docking simulations were performed in Raccoon VS, a graphical interface for preparing AutoDock virtual screenings. The binding energy obtained from docking experiments is reported in Kcal/mol.

2.6. Molecular Simulation Studies

The online server CABS-flex 2.0 was used for the molecular simulations of selected steroidal saponins from EEPPR with the best binding affinities with target receptors following the method suggested previously [30]. The values were set as the default parameter as indicated by the server. The root mean square fluctuation (RMSF) curves were visualized using Jupyter Notebook and matplotlib, a Python package. As a result of the simulations under 100 ns, the backbone root mean square deviations (RMSDs) of protein-ligand structures were examined in detail. The RMSD was measured as the mean distance between the backbone atoms of the protein-ligand structures, and it was derived from the following equation:

$$RMSD = \sqrt{\frac{I}{N}\sum_{i=0}^{N}\delta_i^2}$$

Where, N = total number of atoms applicable in the calculation

δ = the distance between the N pairs of equivalent atoms.

2.7. Analysis of Docked Results

The docked ligands with both the receptors, namely, ERα (PDB ID: 3ERT) and EGFR tyrosine kinase (PDB ID: 1M17) were analyzed in PyMOLv0.99 [27]. The interaction analyses were performed by LigPlot$^+$ software to visualize the active amino acid residues involved in the binding of the atoms of top-hit phytocompounds (ligands) from *P. polyphylla* rhizome. They were compared with the binding of amino acid residues of natural ligands with respective receptors [31]. The amino acids forming hydrogen bonds and those forming hydrophobic interactions were noted.

2.8. Druglikeness Calculations

A Lipinski's rule of five was applied by obtaining the chemical properties and bioactivity prediction provided by the Swiss ADME server to determine if the compounds presented drug-like properties (http://www.swissadme.ch/index.php). The druglikeness was examined with the help of the following attributes: Hydrogen donors (not more than 5), hydrogen bond acceptors (not more than 10), partition coefficient (not more than 5), rotatable bonds (less than 10), total polar surface area (not more than 140), and molecular weight (less than 500 g/mol).

3. RESULTS

3.1. LC–MS Characterization of Phytocompounds

A total of 79 phytocompounds, mostly (non-volatile), were identified from the EEPPR during LC-MS characterization. The LC–MS chromatograms are shown in Figure 2, and the list of compounds obtained is presented in Table 1.

3.2. Selection of Top Hit, Probable Anti-Breast Cancer Phytocompounds, and Binding Energy of Ligands-Receptor Complexes

Our findings in the docking study revealed that the binding energy of the natural ligand erlotinib docked with receptor EGFR tyrosine kinase was −7.1 Kcal/mol and estradiol docked with receptor ERα was −8.1 Kcal/mol [Table 2]. The docking results of top-hit phytocompounds docked from 116 compounds characterized from EEPPR against EGFR tyrosine kinase receptors are presented in Supplementary Table 1a and b. In contrast, that of ERα (PDB ID 3ERT) receptor is given in Supplementary Table 2a and b. It was found that, of the total 116 phytocompounds docked against two breast cancer receptors EGFR tyrosine kinase and ERα, only three phytocompounds (steroidal saponins), namely, diosgenin, pennogenin, and 7-ketodiosgenin acetate, have demonstrated the best binding affinity for the target receptors EGFR tyrosine kinase and ERα which are presented in Table 2 and Figure 3. The binding affinities of the top-hit three phytocompounds (ligands) were found higher when compared with natural ligands (erlotinib and estradiol). These top-hit three phytocompounds (ligands) with higher binding affinities (indicated by lower docking score) were selected and analyzed further. The docking studies of the top hit 03 phytocompounds, namely, diosgenin, pennogenin and 7-ketodiosgenin acetate identified from EEPPR revealed that these phytocompounds (ligands) were strongly bonded to the ligand-binding pocket of each receptor. These docking studies have confirmed that the top-hit three steroidal saponins (diosgenin, pennogenin, and 7-ketodiosgenin acetate) identified from EEPPR could block the natural ligand from binding its target receptor sites which can be used for suppressing the genes that trigger the onset of metastasis.

3.3. Binding Affinity of the Top-Hit Phytocompounds of EEPPR to EGFR Tyrosine Kinase and ERα Receptors

In the present study, diosgenin has demonstrated an excellent binding affinity with target receptor EGFR tyrosine kinase and ERα with a docking score of −9.9 Kcal/mol and −10.1 Kcal/mol, respectively [Table 2]. Diosgenin has already been reported as a significant phytocompounds from *P. polyphylla* of the Eastern Himalayan Region [19]. Meanwhile, pennogenin has shown good binding affinity with receptor protein EGFR tyrosine kinase with a docking score of −10.1 Kcal/mol and also against receptor ERα (3ERT) with a docking score of −9.1 Kcal/mol. The ligand 7-ketodiosgenin acetate showed the highest binding affinity with receptor EGFR tyrosine kinase with a docking score of −11.2 Kcal/mol. It showed a good binding affinity with receptor ERα with a docking score of −10.4 Kcal/mol. The docking score (−11.2 Kcal/mol) of the 7-ketodiosgenin acetate with receptor EGFR tyrosine kinase (1M17) was found to be the best among the docking scores recorded for all the three selected phytocompounds (ligands) binds toward target receptor EGFR tyrosine kinase [Table 2]. All the three steroidal saponins were found to have a higher binding affinity with a low docking score when compared with the docking score (−7.1 Kcal/mol) of the natural ligand – erlotinib when binds with receptor EGFR tyrosine kinase and when compared with docking score (−8.1 Kcal/mol) of another natural ligand – estradiol (E) when binds with receptor ERα.

3.4. Interactions of the Top-Hit Phytocompounds (Steroidal Saponins) of *P. polyphylla* with Amino Acid Residues of the Two Receptors – EGFR Tyrosine Kinase and Erα

LigPlot$^+$ software was used to visualize the active amino acid residues involved in binding of the atoms of top-hit phytocompounds (ligands) from EEPPR and was compared with the binding of amino acid residues of natural ligands with respective receptors (EGFR tyrosine kinase and ERα) and was compared with the amino acids involved when the natural ligand (erlotinib) was used [Table 3]. It was found that among the 17 amino acids involved in the natural ligand (Erlotinib)-receptor

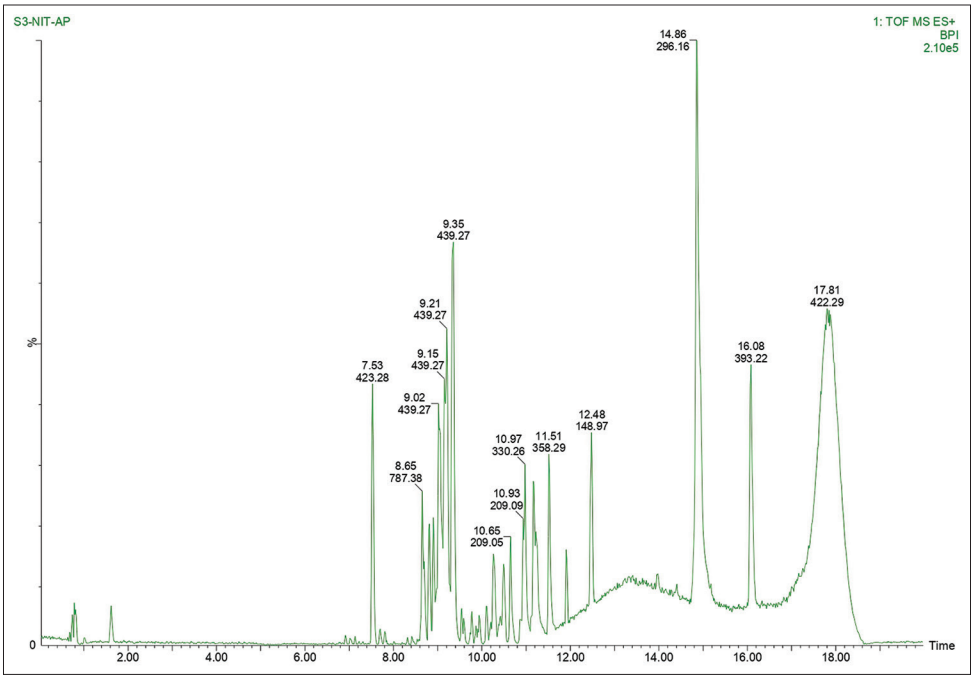

Figure 2: LC–MS chromatogram of phytocompounds obtained from EEPPR. The X-axis represents the time of sample (EEPPR) run while Y-axis shows the area percentage of the phytocompounds. S3 = Sample code for ethanolic extract of *P. polyphylla* rhizome.

Table 2: Docking score of the top-hit three selected phytocompounds (ligands) of steroidal saponin from EEPPR and natural ligands docked against two receptors – EGFR tyrosine kinase and ERα.

Target protein receptors PDB IDs	Docking score of natural ligands (Kcal/mol)	Docking score of selected top-hit phytocompounds (ligands) (Kcal/mol)		
1M17	Erlotinib (A)	Diosgenin	Pennogenin	7-ketodiosgenin acetate
	−7.1	−9.9	−10.1	−11.2
3ERT	Estradiol (E)	Diosgenin	Pennogenin	7-ketodiosgenin acetate
	−8.1	−10.1	−9.1	−10.4

Table 3: Amino acids interaction (hydrophobic binding and polar H binding) of top-hit selected ligands – phytocompounds (diosgenin, pennogenin, and 7-ketodiosgenin acetate) of EEPPR docked with the specific receptors – EGFR tyrosine kinase and ERα. The values were compared with natural ligands (drugs), that is, erlotinib for receptor EGFR and estradiol for receptor ERα.

Target protein receptors PDB IDs	Top-hit phytocompounds (ligands) from *P. polyphylla* and natural ligands	Amino acids with hydrophobic interactions	Hydrogen bonding residues
EGFR tyrosine kinase (1M17)	Diosgenin	Ala719, Asp831, Cys773, Gly772, Leu694, Leu764, Leu820, Lys721, Pro770, Thr766, Thr830, Val702	Glu738, Met742
	Pennogenin	Ala719, Asp831, Cys773, Gly772, Leu694, Leu764, Leu820, Lys721, Pro770, Thr766, Thr830, Val702,	Glu738 Met742
	7-ketodiosgenin acetate	Ala719, Cys773, Gln767, Glu738, Gly772, Leu694, Leu764, Leu768, Leu820, Lys721, Met742, Phe771, Pro770, Thr766, Val702	Met769
	Erlotinib (natural ligand)	Ala719, Asp831, Gln767, Glu738, Gly695, Gly772, Ile765, Leu764, Leu768, Leu694, Leu820, Lys721, Pro770, Thr766, Thr830, Val702	Met769
ERα (3ERT)	Diosgenin	Ala350, Asp351, Cys530, Leu384, Leu346, Leu525, Met343, Phe404, Thr347, Trp383, Val533	ND
	Pennogenin	Ala350, Arg394, Leu391, Leu346, Leu525, Leu384, Leu387, Met343, Met388, Thr347, Trp383	ND
	7-ketodiosgenin acetate	Ala350, Arg394, Leu384, Leu387, Leu346, Leu391, Leu525, Lys529, Met343, Met528, Thr347, Trp383	Cys530
	Estradiol (natural ligand)	Ala350, Gly420, Ile424, Leu346, Leu387, Leu391, Leu525, Met343, Met421, Phe404	Arg394, Glu353, and His524

interaction, only Met 769 was found to form hydrogen bonding with the receptor Erα. In comparison, the other 14 amino acids, namely, Ala719, Asp831, Gln767, Glu738, Gly695, Gly772, Ile765, Leu764, Leu768, Leu694, Leu820, Lys721, Pro770, Thr766, Thr830, and Val702, were

found to form hydrophobic interactions with receptor ERα [Table 3 and Supplementary Figure 1a-c]. In the case of phytocompounds diosgenin and pennogenin, two amino acids, namely, Glu738 and Met742, were found to form hydrogen bonding with receptor EGFR tyrosine kinase. In comparison, 12 amino acids, namely, Ala719, Asp831, Cys773, Gly772, Leu694, Leu764, Leu820, Lys721, Pro770, Thr766, Thr830, and Val702, were formed hydrophobic interactions with the same receptor EGFR tyrosine kinase. However, in the case of 7-ketodiosgenin acetate, only Met769 formed a hydrogen bond with the EGFR tyrosine kinase receptor. At the same time, the other 15 amino acids, namely, Ala719, Cys773, Gln767, Glu738, Gly772, Leu694, Leu764, Leu768, Leu820, Lys721, Met742, Phe771, Pro770, Thr766, and Val702, were found to form hydrophobic interactions with receptor EGFR tyrosine kinase. The detailed interaction analysis of the top-hit phytoconstituents from EEPPR with the amino acid residues of receptor – EGFR tyrosine kinase is summarized in Table 3 and Figure 4a-d.

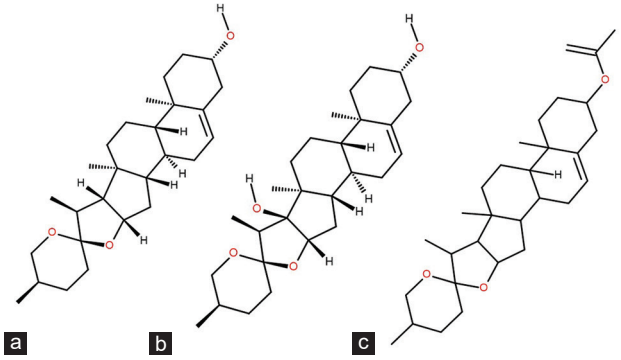

Figure 3: Structure of top-hit three phytocompounds (steroidal saponins) (a) diosgenin (b) pennogenin, and (c) 7-Ketodiosgenin acetate characterized, identified, and docked from ethanolic extract of EEPPR that has demonstrated the highest binding affinity toward the target receptors – EGFR tyrosine kinase and Erα.

Similarly, analysis of active amino acid residues involved in ligand-receptor docking in the case of receptor – ERα was also done [Table 3]. It was found that when the natural ligand (estradiol) was docked with the receptor, a total of 13 amino acids were found actively involved. The three amino acids residues, namely, Arg394, Glu353, and His524, were found to form hydrogen bonding with ERα receptor while the rest 10 amino acids, namely, Ala350, Gly420, Ile424, Leu346, Leu387, Leu391, Leu525, Met343, Met421, and Phe404, have formed hydrophobic interactions with the ERα receptor [Table 3 and Supplementary Figure 1d-f]. In the case of diosgenin, 11 amino acids, namely, Ala350, Asp351, Cys530, Leu384, Leu346, Leu525, Met343, Phe404, Thr347, Trp383, and Val533, were found to form hydrophobic interactions with ERα receptor while in the case of pennogenin, 11 amino acids, namely, Ala350, Arg394, Leu391, Leu346, Leu525, Leu384, Leu387, Met343, Met388, Thr347, and Trp383, were found to form hydrophobic interactions with the ERα receptor while no hydrogen bonding for any of the amino acids with the same receptor. However, in the case of 7-ketodiosgenin acetate, only one amino acid, namely, Cys 530, formed a hydrogen bond with the ERα receptor while other 12 amino acids, namely, Ala350, Arg394, Leu384, Leu387, Leu346, Leu391, Leu525, Lys529, Met343, Met528, Thr347, and Trp383, were found to form hydrophobic interactions with the ERα receptor. The detailed interaction analysis of the top-hit phytoconstituents (diosgenin, pennogenin, and 7-ketodiosgenin acetate) from EEPPR

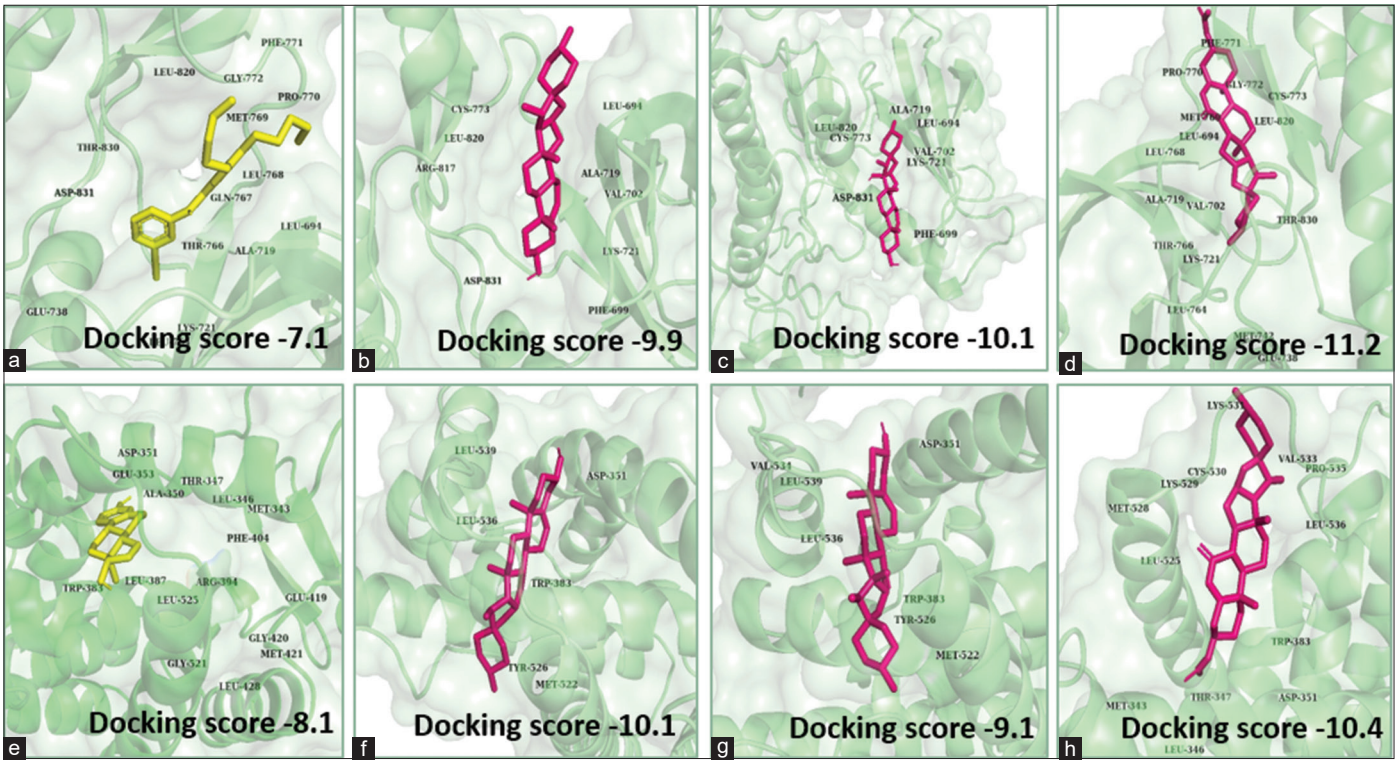

Figure 4: Docking scores of natural ligands (erlotinib and estradiol) and top-hit three phytocompounds (ligands) of EEPPR with selected receptors – EGFR tyrosine kinase and ERα. (a) Erlotinib + EGFR tyrosine kinase, (b) diosgenin + EGFR tyrosine kinase, (c) pennogenin + EGFR tyrosine kinase, (d) 7-ketodiosgenin acetate + EGFR tyrosine kinase, (e) estradiol + ERα, (f) diosgenin + ERα, (g) pennogenin + ERα, and (h) 7-ketodiosgenin acetate + ERα.

with the amino acid residues of the ERα receptor is summarized in Table 3 and Figure 4e-g.

It was also found that the top-hit phytocompounds – steroidal saponins (diosgenin, pennogenin, and 7-ketodiosgenin acetate) of EEPPR utilized a combination of hydrogen bonding and hydrophobic interactions to align themselves more efficiently for binding to the ligand-binding pocket of the target receptors. This strategy ultimately results in an optimal reduction of the system's free energy, which is relatively indicated by the docking scores predicted by Autodock software. The interaction analysis of the top-hit three phytocompounds (steroidal saponins) – diosgenin, pennogenin, and 7-ketodiosgenin acetate with respective EGFR tyrosine kinase and ERα receptors is summarized in Figure 4.

3.5. Comparison of *In silico* Docking of Natural Ligand-Receptor with the Top-Hit Phytocompounds (Steroidal Saponins) of EEPPR

The analysis of docked ligand-receptor complexes revealed that all the top-hit three phytocompounds (of steroidal saponins), namely, diosgenin, pennogenin, and 7-ketodiosgenin acetate from EEPPR, bind at the same junction of the ligand-binding domain of the EGFR tyrosine kinase and ERα receptor kinase domain almost in the same orientation. This was found when the target phytocompounds – diosgenin, pennogenin, and 7-ketodiosgenin acetate were redocked with the complexes of the target receptor with that of its natural ligand. The top-hit three phytocompounds (diosgenin, pennogenin, and 7-ketodiosgenin acetate) as ligand has demonstrated a similar area of interaction despite the presence of the natural ligand albeit with high binding affinity, as shown in Figure 5a-f. It shows that these steroidal saponins (diosgenin, pennogenin, and 7-ketodiosgenin acetate) have a more specific binding affinity with the natural ligand-binding domain of the target receptors which can be used as a potent anti-breast cancer drug. This shows that the diosgenin, pennogenin, and 7-ketodiosgenin acetate present in *P. polyphylla* mimic the binding characteristics of the natural ligands – erlotinib and estradiol with the receptors EGFR tyrosine kinase and ERα, respectively.

3.6. Results of Molecular Simulation Studies for EGFR Tyrosine Kinase and ERα Receptors with the Bonded Ligands

The result of molecular simulation analysis demonstrated a stable and robust binding affinity of all the steroidal saponins, namely, diosgenin, pennogenin, and 7-ketodiosgenin acetate with EGFR tyrosine kinase and ERα receptors. The RMSF curve was found lower than that of natural ligand (denoted in black) in the case of all the three steroidal saponins, namely, diosgenin (green), and pennogenin (red) and 7-ketodiosgenin acetate (blue) at amino acids positions Ala719, Leu694, Lys721, and Thr830. However, it was also found that in addition to these amino acid residues, the RMSF curve of the steroidal saponin 7-ketodiosgenin acetate was found lower in positions Glu738, Gln767, Gly772, Leu764, Leu768, and Leu820 [Figure 6a]. This probably accounts for a more binding affinity of the steroidal saponin 7-ketodiosgenin acetate with the EGFR tyrosine kinase receptor.

Similarly, for the ERα receptor, the RMSF curve was found lower in the case of the top hit 03 phytocompounds, namely, diosgenin, pennogenin, and 7-ketodiosgenin acetate at positions Asp351, Glu353, Gly420, Gly521, Leu346, Leu387, Met343, Phe404, and Trp383. In the case of diosgenin (green) and 7-ketodiosgenin acetate (blue), additional amino acid positions were found to possess lower RMSF values for amino acids Arg394, Glu419, Leu428, Leu525, and Met421 when compared with that of natural ligand estradiol [Figure 6b]. The lower docking scores observed in the case of diosgenin (−10.1 Kcal/mol) and 7-ketodiosgenin acetate (−10.4 Kcal/mol) further supported the present findings [Table 2]. The lower RMSF value shown by a dip in the curves suggested a more stable interaction between the three steroidal saponins (diosgenin, pennogenin, and 7-ketodiosgenin

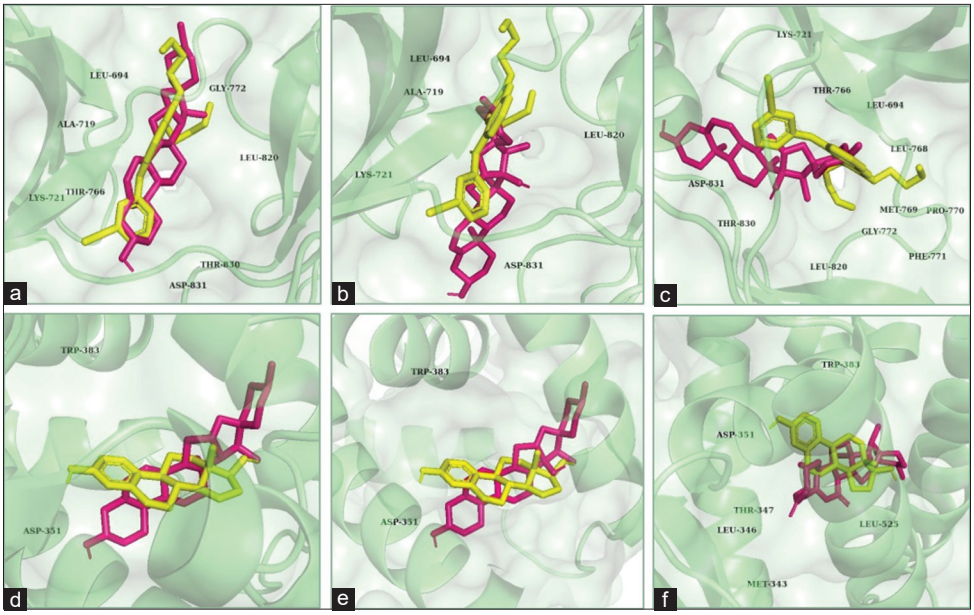

Figure 5: Comparison of natural ligand binding with selected receptors EGFR tyrosine kinase and ERα with that of top-hit three phytocompounds (diosgenin, pennogenin, and 7-ketodiosgenin acetate) from EEPPR (a) EGFR tyrosine kinase + diosgenin + erlotinib, (b) EGFR tyrosine kinase + pennogenin + erlotinib, (c) EGFR tyrosine kinase + 7-ketodiosgenin acetate + erlotinib, (d) ERα + diosgenin + estradiol, (e) ERα + pennogenin + estradiol, and (f) ERα + 7-ketodiosgenin acetate + estradiol. It was found that compared to the natural ligand (shown in yellow), the selected three top-hit phytocompounds (shown in pink) have demonstrated higher affinity (as indicated by docking score) for the target protein receptors which could be used as an anti-breast cancer drug.

acetate) and the target protein receptors. The RMSD average values for EGFR tyrosine kinase and ERα receptors were found at 4.5 ± 0.02 Å and 4.5 ± 0.02 Å, respectively. The ligand-receptor binding complexes were stable throughout the 100 ns of molecular simulation.

3.7. Drug Likeness Calculations for the Top-Hit Phytocompounds (Diosgenin, Pennogenin, and 7-Ketodiosgenin acetate) of *P. polyphylla*

On calculating Lipinski rule of 5 using SWISS-ADME server for the top-hit three steroidal saponins (phytocompounds), namely, diosgenin, pennogenin, and 7-ketodiosgenin acetate of EEPPR, it has been confirmed that pennogenin fulfilled all the required eligibility criteria for rational drug design for oral use. Diosgenin and 7-ketodiosgenin acetate have shown one violation each. The individual molecular weight of the three steroidal saponins and the natural ligands are presented in Table 4.

4. DISCUSSION

The present docking study of 116 phytocompounds selected and docked from *P. polyphylla* rhizome has revealed top hit three steroidal saponins, namely, diosgenin, pennogenin, and 7-Ketodiosgenin acetate as potential anti-breast cancer compounds, which successfully bind with ligand binding sites of their respective two breast cancer receptors – EGFR tyrosine kinase and ERα. Earlier, *P. polyphylla* rhizome from the Eastern Himalayan region of India and China has been reported as a rich source of diosgenin, pennogenin, and polyphyllin (major constituents of steroidal saponins) and has been reported as a potential anti-cancer agent [19,20].

Breast cancer is the most prevalent cancer type and is reported to be responsible for high mortality among the women population across the globe [3,32], with a total global population of 2.3 million in 2020 which represents 11.7% of the global cancer population [33]. The upregulated levels of sex hormones such as estrogen and progesterone may trigger the progression of breast cancer. Hence, checking the overexpression of these sex hormones by replacing them with drug analogues (ligand) that could bind to the receptor sites is fundamental for checking the onset of metabolic pathways that lead to the progression of breast cancer cells [4]. ERα and EGFR tyrosine kinase receptors play a critical role in breast cancer development. Studies have also demonstrated that PRs are significantly elevated if ER is overexpressed because PR is the end product resulting from estrogenic stimulation [6]. On the other hand, EGFR receptors are reported to play a critical role in triple-negative breast cancer cells, that is, cells that are phenotypical ER negative, PR negative, as well as HER-2 negative which limit these cells to be effective against a wide variety of drugs. The current FDA-approved anti-breast cancer drugs, namely, the neratinib, lapatinib, tucatinib, pyrotinib, sunitinib, apatinib, lenvatinib, cabozantinib, pazopanib, axitinib, sorafenib, anlotinib, fruquintinib, cediranib, donafenib, and famitinib which are available in the market are reported with several side effects. Therefore, anti-hormone therapy using phytocompounds from traditional medicinal plants is a promising approach for the treatment of breast cancer [34,35]. In the recent decade, bioinformatics tools and techniques such as molecular docking

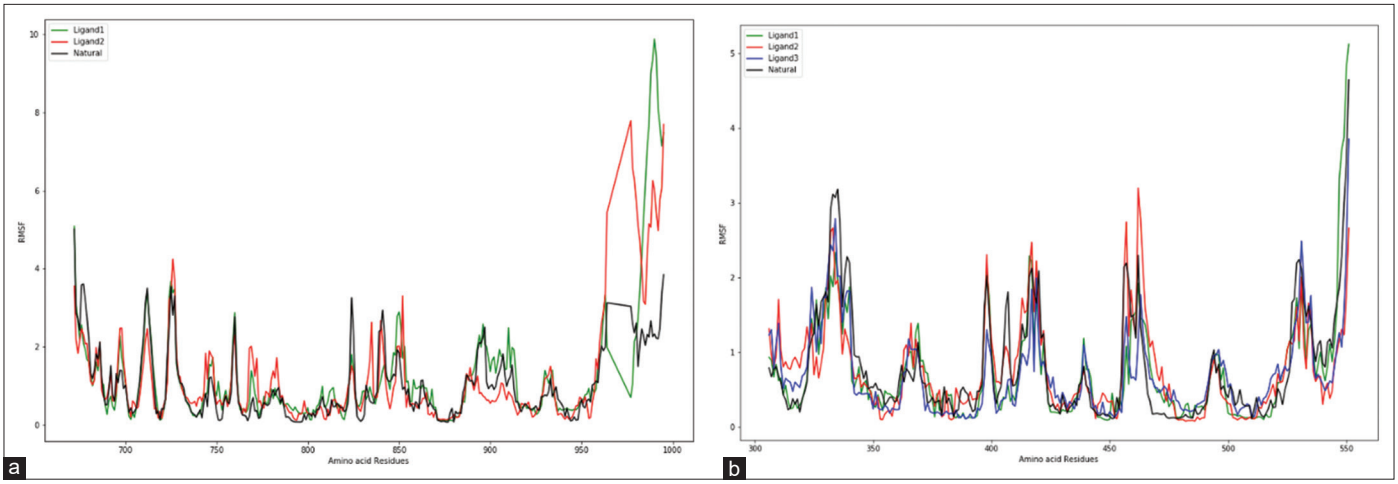

Figure 6: Molecular simulation studies of the top-hit three phytocompounds, namely, diosgenin, pennogenin, and 7-ketodiosgenin acetate of EEPPR using CABS-flex 2.0 for selected proteins receptor (a) ERα receptor and (b) EGFR tyrosine kinase receptor. The curves on the plots were marked with colors: Natural ligand = black, diosgenin (L1) = green, pennogenin (L2) = red, and 7-ketodiosgenin acetate (L3) = blue. The X-axis denotes the position of active amino acids, while the Y-axis denotes RMSF values.

Table 4: *In silico* bioactivity details of the top-hit ligands (anti-breast cancer phytocompounds) – diosgenin, pennogenin, and 7-ketodiosgenin acetate identified from EEPPR along with the two natural ligands (erlotinib and estradiol) of the target receptors – EGFR tyrosine kinase and ERα.

Top-hit ligands	HBD	HBA	MlogP	RB	TPSA	MW	Lipinski violation
Diosgenin	1	3	4.94	0	38.69	414.62	1
Pennogenin	2	4	4.09	0	58.92	430.62	0
7-Ketodiosgenin acetate	0	5	4.26	2	61.83	470.64	1
Erlotinib	1	6	1.48	10	74.73	393.44	0
Estradiol	2	2	3.53	0	40.46	272.38	0

HBD: Hydrogen bond donors (not more than 5), HBA: Hydrogen bond acceptors (not more than 10), MlogP: Partition coefficient (Mlog P < 4.15), RB: Rotatable bonds (less than 10), TPSA: Topological polar surface area (not more than 140), MW: Molecular weight (less than 500 g/mol)

and molecular simulation studies help in the correct identification of phytochemicals as potential receptor TKIs from traditional medicinal plants which can be used for effective treatment of breast and stomach cancer [19,36]. In the present study, diosgenin, pennogenin, and 7-ketodiosgenin acetate docked and identified from EEPPR are found to block the natural ligands (erlotinib and estradiol) from binding the two target receptors (EGFR tyrosine kinase and ERα) sites and thus prevent the overexpression of two breast cancer receptors which can be used for suppressing the genes that trigger the onset of metastasis. However, among the three phytocompounds identified from EEPPR, 7-ketodiosgenin acetate has demonstrated the highest binding affinity with receptor EGFR tyrosine kinase with the lowest docking score of −11.2 Kcal/mol but also demonstrated good binding affinity with receptor ERα with a docking score of −10.4 Kcal/mol.

The interaction analysis of diosgenin, pennogenin, and 7-ketodiosgenin acetate from EEPPR with the amino acid residues of EGFR tyrosine kinase and ERα receptors has revealed that these top-hit three phytocompounds utilized a combination of hydrogen bonding and hydrophobic interactions to align and bind themselves efficiently to the ligand-binding pocket of the target breast cancer receptors. The molecular simulation study further confirmed that the lower RMSF value demonstrated by a dip in the curves indicated stable interaction between the diosgenin, pennogenin, and 7-ketodiosgenin acetate and the target protein receptors. The ligand-receptor binding complexes were found stable throughout the 100 ns of molecular simulation. Results of the present molecular docking and molecular simulation study confirmed that diosgenin, pennogenin, and 7-ketodiosgenin acetate have a more specific binding affinity with the natural ligand-binding domain of the target receptors and they can be used as a potent anti-breast cancer drug. They could also be a potent inhibitors for viral proteases of SARS-CoV-2 [37,38], of this also implies that these three phytocompounds (diosgenin, pennogenin, and 7-ketodiosgenin acetate) from *P. polyphylla* mimic the binding characteristics of the natural ligands – erlotinib and estradiol with the receptors EGFR tyrosine kinase and ERα. A study on Lipinski's rule of 5 has confirmed pennogenin as the best ligand which satisfied all the required eligibility criteria for a rational drug design for oral use, however, diosgenin and 7-ketodiosgenin acetate have demonstrated one violation each but they could also be used for the development of anti-breast cancer drug. Earlier, diosgenin from *P. polyphylla* rhizome has proven effective against some breast cancer cell lines such as MCF7, T47D, and MDA-MB-231 by exerting its anticancer effect following multiple pathways such as apoptosis and inhibition of cancer cells [39], and by inhibiting the overexpressed Vav 2 proteins of breast cancer cells [40]. The diosgenin was also reported to inhibit HER2 positive breast cancer cells by inhibiting the Akt signaling pathway [41,42]. However, *in silico*- and *in vitro*-based anticancer activities of pennogenin and 7-ketodisogenin acetate are not available to date. The present *in silico*-based study confirmed that the three steroidal saponins docked and identified from *P. polyphylla* rhizome have the potential to be developed as novel anti-breast cancer drugs. This has paved the way for further isolation of these three bioactive compounds for *in vitro* and *in vivo* evaluation of their anti-cancer properties.

5. CONCLUSION

Of the total 116 phytocompounds screened and characterized from EEPPR and docked against two breast cancer receptors EGFR tyrosine kinase and ERα, only three phytocompounds (steroidal saponins), namely, diosgenin, pennogenin, and 7-ketodiosgenin acetate, have demonstrated higher binding affinity toward the target breast cancer receptors. Diosgenin has shown the highest binding affinity with receptor ERα with a docking score of −10.1 Kcal/mol and pennogenin has shown the highest binding affinity with receptor EGFR tyrosine kinase with a docking score of −10.1 Kcal/mol. The binding affinity of all the three steroidal saponins was found higher with a low docking score when compared with the docking score (−7.1 Kcal/mol) of the natural ligand (erlotinib) when binding with receptor EGFR tyrosine kinase and docking score (−8.1 Kcal/mol) of another natural ligand (estradiol) when binds with receptor ERα. The interaction analyses of amino acid residues of ligand-receptor complexes revealed that the selected three steroidal saponins utilized a combination of hydrogen bonding and hydrophobic interactions. The molecular simulation analysis confirmed that the lower RMSF value shown by a dip in the curves indicated stable interaction between diosgenin, pennogenin, and 7-ketodiosgenin acetate their respective target receptors while the ligand-receptor complexes were found stable throughout the 100 ns of molecular simulation. Application of Lipinski rule of 5 using Swiss-ADME server has confirmed pennogenin as the best phytocompound (ligand) which fulfilled all the required eligibility criteria for rational drug design for oral use while diosgenin and 7-ketodiosgenin acetate have demonstrated one violation each. The present findings suggested that these steroidal saponins identified and docked from *P. polyphylla* rhizome could be used as potential ligands (inhibitors) against the EGFR tyrosine kinase and ERα receptors. This has conferred further opportunities for isolation, *in vivo* and *in vitro* study of the pennogenin from *P. polyphylla* rhizome for the development of alternative anti-breast cancer drugs.

6. STATEMENT OF DISCLOSURE

The authors hereby declare that they have no conflicts of interest.

7. ACKNOWLEDGMENTS

The corresponding author (PKH) is thankful to Science and Engineering Research Board (SERB), Department of Science and Technology (DST), New Delhi, Ministry of Science and Technology, Govt. of India, for funding support to the present work through the ECR scheme vide grant No. ECR/2016/001626 dated March 22, 2017. The authors are thankful to Mr. Arshad Khan and Mr. Satyam Sangeet for helping in carrying out the ADME and molecular simulation studies. The much needed logistic support extended by the Director of NIT Arunachal Pradesh, Yupia, and Vice-Chancellor of Rajiv Gandhi University, Rono Hills, Doimukh, Arunachal Pradesh, are deeply acknowledged.

8. AUTHORS' CONTRIBUTIONS

All authors made substantial contributions to conception and design, acquisition of data, or analysis and interpretation of data; took part in drafting the article or revising it critically for important intellectual content; agreed to submit to the current journal; gave final approval of the version to be published; and agreed to be accountable for all aspects of the work. All the authors are eligible to be an author as per the International Committee of Medical Journal Editors (ICMJE) requirements/guidelines.

9. CONFLICTS OF INTEREST

The authors report no financial or any other conflicts of interest in this work.

10. ETHICAL APPROVALS

This study did not involve animal experiment; therefore, approval of institutional animal ethical committee (IAEC) was not required.

11. DATA AVAILABILITY

All the vital findings related to this study has been provided as both main and supplementary data.

12. PUBLISHER'S NOTE

This journal remains neutral with regard to jurisdictional claims in published institutional affiliation.

REFERENCES

1. Pérez-Herrero E, Fernández-Medarde A. Advanced targeted therapies in cancer drug nanocarriers, the future of chemotherapy. Eur J Pharm Biopharm 2015;1:52-79.
2. DeSantis CE, Ma J, Gaudet MM, Newman LA, Miller KD, Sauer AG, *et al.* Breast cancer statistics 2019. CA Cancer J Clin 2019;69:438-51.
3. Siegel RL, Miller KD, Jemal A. Cancer statistics, 2019. CA Cancer J Clin 2019;69:7-34.
4. Waks AG, Winer EP. Breast cancer treatment: A review. JAMA 2019;321:288-300.
5. Persson I. Estrogens in the causation of breast, endometrial and ovarian cancers-evidence and hypotheses from epidemiological findings. J Steroid Biochem Mol Biol 2000;74:357-64.
6. Acharya R, Chacko S, Bose P, Lapenna A, Pattanayak SP. Structure-based multitargeted molecular docking analysis of selected furanocoumarins against breast cancer. Sci Rep 2019;9:1-13.
7. Jordan VC. The new biology of estrogen-induced apoptosis applied to treat and prevent breast cancer. Endocr Relat Cancer 2014;22:R1-31.
8. Levin ER. Bidirectional signalling between the estrogen receptor and the epidermal growth factor receptor. J Mol Endocrinol 2003;17:309-17.
9. Wee P, Wang, Z. Epidermal growth factor receptor cell proliferation signalling pathways. Cancers 2017;9:52.
10. Paul MR, Pan TC, Pant DK, Shih NN, Chen Y, Harvey KL, *et al.* Genomic landscape of metastatic breast cancer identifies preferentially dysregulated pathways and targets. J Clin Invest 2020;130:4252-65.
11. Nouri Z, Fakhri S, Nouri K, Wallace CE, Farzaei MH, Bishayee A. Targeting multiple signalling pathways in cancer: The rutin therapeutic approach. Cancers (Basel) 2020;12:2276.
12. Govaerts R. World Checklist of Melanthiaceae. Facilitated by the Royal Botanic Gardens, Kew; 2020. Available from: http://wcsp.science.kew.org [Last accessed on 2020 Aug 22].
13. Wang J, Li D, Ni W, Qin XJ, Liu H, Yu LL, *et al.* Molecular networking uncovers steroidal saponins of Paris tengchongensis. Fitoterapia 2020;145:104629.
14. Paul A, Gajurel PR, Das AK. Threats and conservation of *Paris polyphylla* an endangered, highly exploited medicinal plant in the Indian himalayan region. Biodiversitas 2015;16:295-302.
15. Gupta DD, Mishra S, Verma SS, Shekher A, Rai V, Awasthee N, *et al*. Evaluation of antioxidant, anti-inflammatory and anticancer activities of diosgenin enriched *Paris polyphylla* rhizome extract of Indian himalayan landraces. J Ethnopharmacol 2021;270:113842.
16. Sharma A, Kalita P, Tag H. Distribution and phytomedicinal aspects of *Paris polyphylla* Smith from the Eastern Himalayan region: A review. Tang Hum Med 2015;5:1-15.
17. Das SK, Das TJ, Tshering D, Tsering J, Paul D, Gupta DD, *et al.* Ethnobotanical notes on significant food and medicinal flora used by the indigenous Monpa and Nyishi communities of Arunachal Pradesh, India. Pleione 2019;13:291-304.
18. Kohara A, Nakajima C, Hashimoto K, Ikenaga T, Tanaka H, Shoyama Y, *et al.* A novel glucosyltransferase involved in steroid saponin biosynthesis in *Solanum aculeatissimum*. Plant Mol Biol 2005;57:225-39.
19. Paul D, Mahanta S, Tag H, Das SK, Das Gupta D, Tanti B, *et al.* Identification of tyrosine kinase inhibitors from *Panax bipinnatifidus* and *Panax pseudoginseng* for RTK-HER2 and VEGFR2 receptors, by *in silico* approach. Mol Divers 2021;23:1-23.
20. Fu YL, Zhao ZH, Shan YJ Cong YW. Inducing effect of total steroid saponins from *Paris polyphylla* on platelet aggregation *in vitro* and its potential mechanism. Bull Acad Mil Med Sci 2007;31:416.
21. Forli S, Huey R, Pique ME, Sanner MF, Goodsell DS, Olsonet AJ. Computational protein-ligand docking and virtual drug screening with the AutoDock suite. Nat Protoc 2016;11:905-19.
22. Plants of the World Online. Royal Botanic Garden, Kew: United Kingdom. Available from: http://www.plantsoftheworldonline.org [Last accessed on 2021 Sep 10].
23. Horai H, Arita M, Kanaya S, Nihei Y, Ikeda T, Suwa K, *et al*. MassBank: A public repository for sharing mass spectral data for life sciences. J Mass Spectrom 2010;45:703-14.
24. Tautenhahn R, Cho K, Uritboonthai W, Zhu Z, Patti GJ, Siuzdak G. An accelerated workflow for untargeted metabolomics using the METLIN database. Nat Biotechnol 2012;30:826-8.
25. Wishart DS, Knox C, Guo AC, Eisner R, Young N, Gautam B, *et al.* HMDB: A knowledge base for the human metabolome. Nucleic Acids Res 2009;37:603-10.
26. Duke J. Dr Duke's Phytochemical and Ethnobotanical Databases. Data Extent: Ag Data Commons; 2018. Available from: http://www.ars-grin.gov/duke [Last accessed on 2021 Sep 15].
27. National Center for Biotechnology Information (NCBI). United States of America [Last accessed on 2021 Aug 25].
28. Schrodinger LLC. The PyMOL Molecular Graphics System, Version 1.3r1; 2010.
29. Morris GM, Huey R, Lindstrom W, Sanner MF, Belew RK, Goodsell DS, *et al.* AutoDock4 and AutoDockTools4: Automated docking with selective receptor flexibility. J Comput Chem 2009;30:2785-91.
30. Kuriata A, Gierut AM, Oleniecki T, Ciemny MP, Kolinski A, Kurcinski M, *et al.* CABS-flex 2.0: A web server for fast simulations of flexibility of protein structures. Nucleic Acids Res 2018;46:338-43.
31. Wallace AC, Laskowski RA, Thornton JM. Ligplot: A program to generate schematic diagrams of protein-ligand interactions. Protein Eng Des Sel 1995;8:127-34.
32. Du XL, Fox EE, Lai D. Competing causes of death for women with breast cancer changed over time from 1975 to 2003. Am J Clin Oncol 2008;31:105-16.
33. Sung H, Ferlay J, Siegel RL, Laversanne M, Soerjomataram I, Jemal A, *et al*. Global cancer statistics 2020: GLOBOCAN estimates of incidence and mortality worldwide for 36 cancers in 185 countries. CA Cancer J Clin 2021;71:209-249.
34. Nagini S. Breast cancer: Current molecular therapeutic targets and new players. Anticancer Agents Med Chem 2017;17:152-63.
35. Sun Q, Lin X, Zhao Y, Li L, Yan K, Liang D, *et al*. Deep learning vs. Radiomics for predicting axillary lymph node metastasis of breast cancer using ultrasound images: Don't forget the peritumoral region. Front Oncol 2020;10:53.
36. Das SK, Deka SJ, Paul D, Gupta DD, Das TJ, Maravi DK, *et al*. *In-silico* based identification of phytochemicals from *Houttuynia cordata* Thunb. As potential inhibitors for overexpressed HER2 and VEGFR2 cancer genes. J Biomol Struct Dyn 2021;1-14.
37. Gogoi B, Chowdhury P, Goswami N, Gogoi N, Naiya T, Chetia P, *et al.* Identification of potential plant-based inhibitor against viral proteases of SARS-CoV-2 through molecular docking, MM-PBSA binding energy calculations and molecular dynamics simulation. Mol Divers 2021;25:1963-77.
38. Gogoi M, Borkotoky M, Borchetia S, Chowdhury P, Mahanta S, Barooah AK. Black tea bioactives as inhibitors of multiple targets of

SARS-CoV-2 (3CLpro, PLpro and RdRp): A virtual screening and molecular dynamic simulation study. J. Biomol Struct 2021;5:1-24.
39. Bhuvanalakshmi G, Basappa, Rangappa KS, Dharmarajan A, Sethi G, Kumar AP, *et al*. Breast cancer stem-like cells are inhibited by diosgenin, a steroidal saponin, by the attenuation of the Wnt β-catenin signalling via the Wnt antagonist secreted frizzled-related protein-4. Front Pharmacol 2017;8:1-14.
40. He Z, Chen H, Li G, Zhu H, Gao Y, Zhang L, *et al.* Diosgenin inhibits the migration of human breast cancer MDA-MB-231 cells by suppressing Vav2 activity. Phytomedicine 2014;21:871-6.
41. Chiang CT, Way TD, Tsai SJ, Lin JK. Diosgenin, a naturally occurring steroid, suppresses fatty acid synthase expression in HER2-overexpressing breast cancer cells through modulating Akt, mTOR and JNK phosphorylation. FEBS Lett 2007;581:5735-42.
42. Srinivasan S, Koduru S, Kumar R, Venguswamy G, Kyprianou N, Damodaran C. Diosgenin targets Akt-mediated prosurvival signalling in human breast cancer cells. Int J Cancer 2009;125:961-7.

How to cite this article:
Gupta DD, Mahanta S, Das SG, Das SK, Paul D, Tag H, Hui PK. Identification of phytocompounds from *Paris polyphylla* Smith as potential inhibitors against two breast cancer receptors (Erα and EGFR tyrosine kinase) through chromatographic and *in silico* approaches. J App Biol Biotech. 2022;10(6):60-80. DOI: 10.7324/JABB.2022.100607

SUPPLEMENTARY

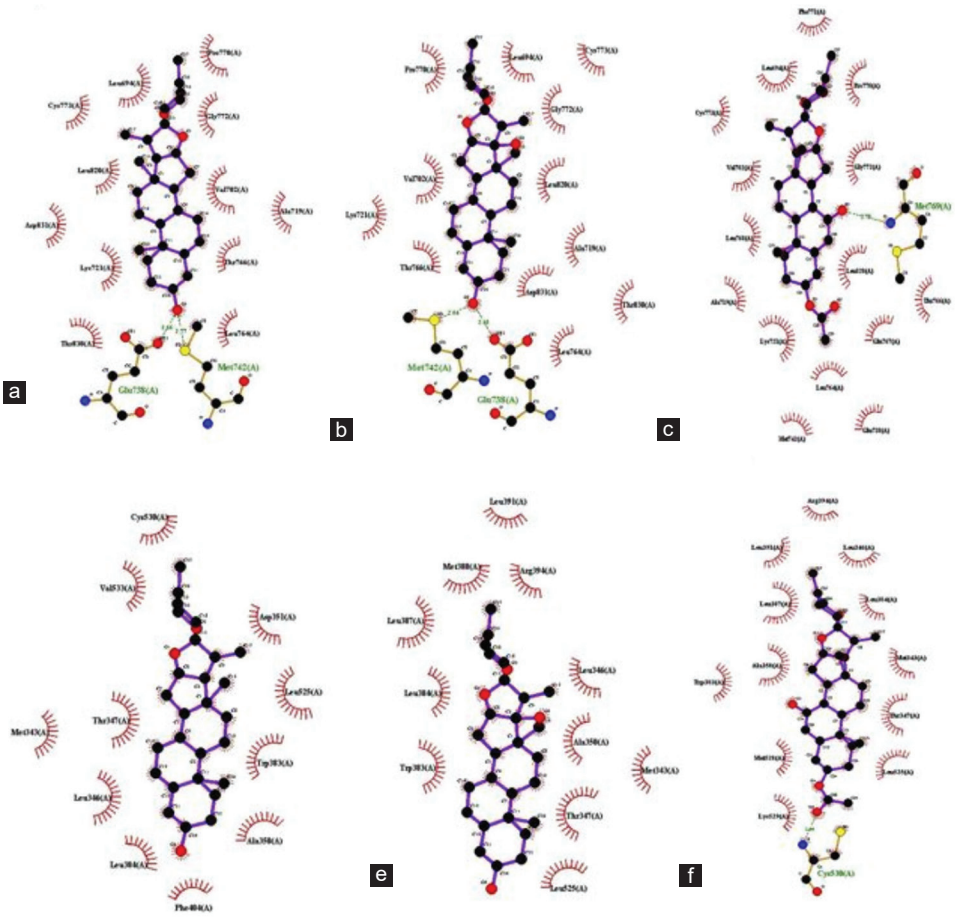

Supplementary Figure 1: (a-f) Interactions of the ligands with the receptors.

Supplementary Table 1a: Docking results of phytoconstituents obtained from GC–MS characterization of EEPPR docked with EGFR tyrosine kinase receptor.

S. No.	Compound Name	Binding energy (Kcal/mol)	Binding residues	Hydrogen bonding residues
1.	1,1-Dimethoxypropane	−3.8	Met742, Thr830, Leu820, Glu738, Thr766, Lys721, Leu764, Asp831	ND
2.	3-(2-Methoxyethoxymethoxy)-2-methylpentan-1-ol	−4.9	Leu768, Leu820, Val702, Leu694, Glu738, Asp831, Lys721, Thr830, Ala719, Thr766, Met742, Met769	Met769
3.	1,3-Diethoxy-2-propanol	−4.3	Thr766, Met742, leu764, Phe699, Thr830, Asp831, Lys721	Thr830, Asp831, Lys721
4.	2-(1-Ethoxyethoxy)-2-(2-oxiranyl) ethanol	−4.7	Ala719, Leu964, Leu820, Val702, Cys773, Arg817, Phe699, Asn818, Leu834, Gly833, Lys721, Asp831	ND
5.	Diethoxymethane	−3.6	Lys721, Ala719, Thr830, Leu764, Met742, Thr766, Val720	ND
6.	1,1,3-Triethoxypropane	−4.4	Lys721, Thr766, Thr830, Leu694, Ala719, Leu768, Leu820, Gln767, Val702, Met769	Met769
7.	1,1,3-triethoxybutane	−4.4	Met742, Lys721, Thr830, Asp831, Val702, Leu820, Ala719, Leu764, Thr766	ND
8.	D-allose	−5.8	Met743, Leu840, Val702, Lys731, Ile765, Leu764, Glu738, Thr830, Asp831, Ala719, Thr766	Leu764, Glu738, Thr830, Asp831, Ala719, Thr766
9.	Methyl palmitate	−4.8	Ala719, Leu820, Met742, Thr766, Thr830, Asp831, Arg817, Cys773, Val702, Met769, Leu764	ND
10.	Palmitic acid	−5.1	Ala719, Val702, Gly772, Leu820, Met769, Leu764, Thr766, Glu738, Thr830, Asp831, Lys721	Asp831, Lys721
11.	Ethyl palmitate	−5.2	Leu694, Val702, Thr830, Ala719, Glu738, Leu764, Met742, Lys721, Thr766, Leu820, Met769, Asp831	Asp831
12.	Trimethylsilyl palmitate	−5.2	Leu82076, Asp831, Phe699, Gly833, Glu734, Glu738, Ile735, Lys721, Leu723, Thr766, Val702	ND
13.	Methyl linoleate	−5.4	Ala719, Thr766, Glu738, Lys721, Phe699, Met742, Asp831, Gly695, Leu694, Leu820, Val702, Gln767, Gly772, Met769	Met769
14.	3,6-Octadecadienoic acid, methyl ester	−5.2	Val702, Leu694, Leu820, Gly772, Thr766, Thr830, Glu738, Lys721, Phe669, Asp831, Gly695	ND
15.	Linoleic acid	−5.6	Ala719, Met742, Thr766, Thr830, Asp831, Phe699, Leu694, Leu820, Val702, Glu738, Lys721	Glu738, Lys721
16.	(R)-(-)-14-Methyl-8-hexadecyn-1-ol	−5.4	Leu764, Lys721, Asp831, Leu820, Val702, Leu694, Leu768, Ala719, Thr766, Met769	Met769
17.	trans, trans-9,12-Octadecadienoic acid, propyl ester	NA	Conformer generation is disallowed since too flexible	NA
18.	Dichloroacetic acid, tridec-2-ynyl ester	−5.2	Met742, Thr530, Leu320, Thr766, Met769, Leu764, Lys738, Val732, Leu694, Asp831	ND
19.	Ethyl stearate	−5.3	Phe699, Leu723, Lys721, Glu738, Leu764, Met742, Ile720, Ala719, Val702, Thr766, Asp831	ND
20.	Trimethylsilyl (9Z,12Z)-9,12-octadecadienoate	−5.0	Phe699, Asp831, Val702, Thr830, Lys721, Thr766, Ala719, Leu820, Met769, Cys773, Arg817	ND
21.	Trimethylsilyl (5Z,8Z,11Z)-5,8,11-icosatrienoate	−6.1	Leu834, Phe699, Leu694, Val702, Leu820, Thr766, Asp831, Met742, Leu764, Lys721	Lys721
22.	Stearoxytrimethylsilane	−5.2	Val702, Asp831, Phe699, Glu738, Thr766, Ala719, Leu820, Lys721	Lys721
23.	2-Oxiranylmethyl palmitate	−5.0	Gly695, Val702, Lys721, Asp831, Met742, Glu738, Thr830, Thr766, Ile720, Ala719, Leu820, Leu694	ND
24.	Trimethylsilyl (5Z,8Z)-7,7-dimethyl-5,8-icosadienoate	−5.5	Gly695, Gly772, Leu820, Ala719, Lys721, Asp831, Arg817, Phe699, Leu768, Val702, Leu694, Met769	ND
25.	Trimethylsilyl tetracosanoate	−5.6	Leu768, Gly772, Met769, Lys721, Val702, Asp813, Lys851, Leu834, Phe699, Asp831, Ala719, Thr766, Leu694, Leu820, Arg817	Arg817

(Contd...)

Supplementary Table 1a: *(Continued)*

S. No.	Compound Name	Binding energy (Kcal/mol)	Binding residues	Hydrogen bonding residues
26	Stigmasta-4,7,22-trien-3-α-ol	−9.0	Leu694, Gly772, Cys773, Met769, Lys721, Phe699, Asp831, Val702, Ala719, Leu820, Asp831	Asp831
27	7β-Dehydrodiosgenin	NA	Conformer generation is disallowed since too flexible	NA
28.	Stigmast-5-en-3-ol	−8.1	Leu723, Lys730, Lys851, Asn818, Cys773, Arg817, Leu694, Leu820, Asp831, Met769, Ala719, Glu738, Thr766, Thr830, Val702, Lys721, Phe699, Ala698, Ala731, Glu734	ND
29.	Stigmast-5-en-3-yl (9Z)-9-octadecenoate	−8.1	Leu723, Lys730, Lys851, Asn818, Cys773, Arg817, Leu694, Leu820, Asp831, Met769, Ala719, Glu738, Thr766, Thr830, Val702, Lys721, Phe699, Ala698, Ala731, Glu734	ND
30.	Trimethyl (octacosyloxy) silane	−5.5	Ala719, val720, Met769, Gly722, Leu764, Phe699, Leu834, Asp813, Lys851, Arg817, Asp831, Thr830, Glu738, Lys721, Met742, Thr766, Leu764, Leu820	ND
31.	3β -Acetoxystigmasta-4,6,22-triene	−9.1	Ala719, Thr830, Val702, Lys721, Asp813, Pro853, Leu834, Lys851, Arg817, Phe699, Asp831, Leu820, Thr766	ND
32.	Silane, trimethyl (stigmasta-5,22-dien-3beta-yloxy)	−9.0	Thr766, Ala719, Val702, Lys721, Phe699, Lys851, Pro853, Asp813, Asp831, Thr830, Leu820	ND
33.	Diosgenin	−9.9	Ala719, Asp831, Cys773, Gly772, Leu694, Leu764, Leu820, Lys721, Pro770, Thr766, Thr830, Val702	Glu738, Met742
34.	Stigmast-5-ene, 3 beta-(trimethylsiloxy), (24S)	−9.0	Thr766, Leu820, Thr830, Lys721, Phe699, Asp813, Lys851, Pro853, Asp831, Val702, Ala719	ND
35.	7-Ketodiosgenin acetate	−11.2	Pro770, Gly772, Cys773, Leu768, Ala719, Thr766, Leu820, Leu764, Met742, Lys721, Thr830, Glu738, Val702, Phe771, Leu694, Met769	Met769
36.	7 β-hydroxydiosgenin	NA	Conformer generation is disallowed since too flexible	NA
37.	Pennogenin	−10.1	Ala719, Asp831, Cys773, Gly772, Leu694, Leu764, Leu820, Lys721, Pro770, Thr766, Thr830, Val702	Glu738 Met742

Supplementary Table 1b: Docking results of phytoconstituents obtained from LC–MS characterization of EEPPR docked with EGFR tyrosine kinase receptor.

S. No.	Compound name	Binding energy (Kcal/mol)	Binding residues	Hydrogen bonding residues
1.	2,5-Dimethoxycinnamic acid	−6.3	Leu820, Met769, Ile765, Leu764, Thr766, Lys721, Val702, Asp831, Ala719	Ala719
2.	Kaempferol	−6.1	Leu768, Gly772, Leu820, Leu694, Thr766, Thr830, Asp831, Glu738, Ala719, Met769, Lys721	Met769, Lys721
3.	2-Benzylsuccinic acid	−6.6	Leu764, Met742, Thr830, Leu820, Val702, Thr766, Ile765, Ile720, Ala719, Glu738, Lys721	Ala719, Glu738, Lys721
4.	Sinapyl aldehyde	−6.2	Thr766, Thr830, Lys721, Phe699, Asn818, Asp831, Val702, Met742	ND
5.	6-Methoxymellein	−7.0	Thr766, Ala719, Lys721, Val702, Leu694, Gly772, Leu820, Leu768, Gln767, Met769	Gln767, Met769
6.	2-Benzylsuccinate	−6.7	Met742, Thr766, Leu764, Leu820, Val702, Thr830, Asp831, Glu738, Lys721	Asp831, Glu738, Lys721
7.	5-[(3,4-Dihydroxyphenyl) methyl] oxolan-2-one	−6.9	Glu738, Thr766, Met742, Thr830, Leu764, Val702, Leu820, Ala719, Leu768, Met769, Gln767	Met769, Gln767
8.	Furapiole	−6.7	Leu820, Glu738, Asp831, Thr830, Thr766, Lys721, Ala719, Val702	ND
9.	1-(2-Methoxy-3,4-methylenedioxyphenyl)-1-propanone	−5.7	Glu738, Lys721, Thr766, Leu694, Ala719, Val702, Leu820, Asp831, Thr830	ND

(Contd...)

Supplementary Table 1b: *(Continued)*

S. No.	Compound name	Binding energy (Kcal/mol)	Binding residues	Hydrogen bonding residues
10.	4-Methyl-4-aza-5-pregnene-3,20-dione	-7.8	Gly772, Met769, Cys773, Val702, Asp831, Thr830, Glu738, Ala719, Leu820, Pro770, Leu694, Lys721	Lys721
11.	Butanedioic acid	−5.8	Thr530, Leu620, Thr766, Thr764, Lys721	ND
12.	Gallic acid	−6.2	Glu738, Lys721, Thr766, Leu694, Ala719, Val702, Leu820, Asp831, Thr830	Leu820
13	Chlorogenic acid	−6.5	Thr766, Thr766, Thr830, Lys721, Phe699, Asp831, Val702, Met742	Met742,
14.	Sumatriptan	−6.7	Met769, Gly772, Asp831, Leu694, Leu820, Val702, Lys721, Thr830, Met742, Thr766	ND
15.	4-(8, 9-Dihydro-8-methyl-7H-1, 3-dioxolo (4,5-H) (2,3) benzodiazepin-5-yl) benzenamine	−4.9	Thr830, Leu820, Leu820, Val702, Glu738, Ala719	Glu738
16.	Tetrahydrothiophene-2-carboxylic acid	−4.4	Met742, Thr766, Thr830, Asp831, Lys721	Thr830, Asp831, Lys721
17.	3-methyl sulfolene	−4.8	Thr830, Leu820, Thr766, Leu764, Lys721	ND
18.	3-Oxo-3-ureidopropanoate	−5.2	Leu820, Thr830, Lys721, Val702, Thr766, Ala719, Leu764	Thr766, Ala719, Leu764
19.	5-N-Methyloxaluric acid	−5.1	Leu820, Ala719, Asp831, Met742, Thr830, Thr766, Val702, Lys721, Glu738	Lys721, Glu738
20.	3-Hydroxy-3-methyl-glutaric acid	−5.4	Lys721, Ile765, Thr830, Leu764, Thr766, Ala719, Asp831, Glu738	Ala719, Asp831, Glu738
21.	Levoglucosan	−5.3	Thr830, Ala719, Leu820, Val702, Lys721, Thr766	Thr766
22.	2-Hydroxyadipic acid	−5.1	Asp831, Met742, Val702, Lys721, Thr766, Ala719, Leu764	Lys721, Thr766, Ala719, Leu764
23.	3,3-diethoxy-1-propanol	−4.8	Thr830, Ala719, Ile720, Lys721, Met742, Asp831, Thr766, Leu764, Glu738	Asp831, Thr766, Leu764, Glu738
24.	2S-Hydroxy-hexanedioic acid	−5.1	Ile720, Val702, Leu820, Met742, Thr766, Ala719, Asp831, Thr830, Lys721, Glu738	Asp831, Thr830, Lys721, Glu738
25.	3-Hydroxymethyl-glutaric acid	−5.4	Asp831, Met742, Thr830, Val702, Ile765, Glu738, Lys721, Thr766, Ala719, Leu764	Glu738, Lys721, Thr766, Ala719, Leu764
26.	L-Rhamnono-1,4-lactone	−5.2	Ala719, Leu820, Thr830, Met742, Asp831, Lys721, Glu738, Thr766, Gln767	Lys721, Glu738, Thr766, Gln767
27.	2-Dehydro-3-deoxy-L-rhamnonate	−5.5	Ile765, Glu738, Met742, Thr830, Leu764, Ala719, Asp831, Lys721, Thr766	Ala719, Asp831, Lys721, Thr766
28.	2-Dehydro-3-deoxy-D-fuconate	−4.8	Leu820, Thr830, Thr766, Lys721, Asp831	Lys721, Asp831
29.	(R)-2-Ethylmalate	−5.2	Leu820, Met742, Leu764, Thr766, Lys721, Thr830, Asp831	Lys721, Thr830, Asp831
30.	5-Ureido-4-imidazole carboxylate	−5.8	Val720, Ile720, Leu764, Leu820, Ala719, Asp831, Thr830, Thr766, Lys721	Asp831, Thr830, Thr766, Lys721
31.	Magnesium propionate	−1.4	Asn818, Asp831, His811, Asp813	ND
32.	1-Naphthoic acid	−7.3	Leu764, Val702, Ala719, Thr830, Met742, Thr766, Lys721, Glu738, Asp831	Lys721, Glu738, Asp831
33.	Menadoine	−7.1	Leu764, Lys721, Ala719, Val702, Leu820, Thr830, Glu738, Thr766, Asp831	Asp831
34.	Dehydromatricaria ester	−4.7	Thr766, Thr830, Leu820, Val702, Phe699, Gly695	ND
35.	Methyl (Z)-dec-2-en-4,6,8-triynoate	−5.2	Met769, Thr766, Gly772, Leu820, Ala719, Leu764, Met742, Thr830, Lys721, Asp831, Val702, Leu694, Glu738	Glu738
36.	1-Hydroxy-2-naphthaldehyde	−6.7	Met742, Thr766, Leu764, Val702, Lys721, Thr830, Leu820, Glu738, Asp831	Asp831
37.	2-Naphthoic acid	−6.7	Leu820, Val702, Ala719, Thr766, Thr830, Asp831, Lys721	Asp831, Lys721

(Contd...)

Supplementary Table 1b: *(Continued)*

S. No.	Compound name	Binding energy (Kcal/mol)	Binding residues	Hydrogen bonding residues
38.	3Z-Undecene-5,7,10-triynoic acid	−5.7	Val702, Thr766, Leu764, Ala719, Ile720, Lys721, Asp831, Phe699	ND
39.	4E-Undecene-6,8,10-triynoic acid	−5.8	Lys721, Val702, Ala719, Leu768, Asp831, Phe699, Leu820, Met769	Met769
40.	L-Ascorbic acid	−5.6	Leu764, Thr830, Ala719, Leu820, Met742, Asp831, Glu738, Gln737, Thr766, Lys721	Asp831, Glu738, Gln737, Thr766, Lys721
41.	2-Ketogulonolactone	−5.1	Leu820, Ala719, Asp831, Met742, Thr830, Thr766, Val702, Lys721, Glu738	Lys721, Glu738
42.	Glucuronolactone	−5.1	Val702, Leu820, Thr766, Thr830, Asp831, Lys721	Thr830, Asp831, Lys721
43.	5-Dehydro-4-deoxy-D-glucuronate	−4.6	Leu820, Val702, Glu738, Leu764, Met742, Thr766, Thr830, Asp831, Lys721	Thr830, Asp831, Lys721
44.	(4S)-4,6-Dihydroxy-2,5-dioxohexanoate	−5.3	Ile765, Val702, Ile720, Glu738, Met742, Asp831, Thr830, Leu820, Ala719, Thr766, Leu764, Lys721	Ala719, Thr766, Leu764, Lys721
45.	2-Hydroxy-3-oxoadipate	−5.4	Thr766, Val702, Leu820, Met742, Ala719, Leu764, Glu738, Lys721, Asp831, Thr830	Ala719, Leu764, Glu738, Lys721, Asp831, Thr830
46.	2-Hydroxydibenzofuran	−7.5	Ala719, Leu820, Thr766, Thr830, Asp831, Lys721, Glu738	Lys721, Glu738
47.	Dibenzo-p-dioxin	−6.9	Glu738, Lys721, Met742, Thr830, Thr766, Asp831, Leu820, Ala719, Met769, Gln767	ND
48.	4-Hydroxy-4-methyl-2-oxoglutaric acid	−5.1	Asp831, Met742, Thr766, Leu820, Lys721, Thr830	Lys721, Thr830
49.	D-Glucurono-6,2-lactone	−5.5	Leu820, Ala719, Lys721, Asp831, Thr830, Thr766	Lys721, Asp831, Thr830, Thr766
50.	(4S,5S)-4,5-Dihydroxy-2,6-dioxohexanoate	−6.2	Val702, Leu820, Met742, Thr830, Thr766, Asp831, Ala719, Met769, Gln767	ND
51.	D-Galacturonolactone	−5.3	Ala719, Met742, Thr830, Asp831, Lys721, Thr766	Thr830, Asp831, Lys721, Thr766
52.	4-Hydroxybenzophenone	−7.3	Leu764, Ile720, Lys721, Phe699, Asp831, Val702, Thr830, Thr766, Ile765, Ala719	Ala719
53.	Splitomicin	−7.7	Gln767, Ala719, Met769, Leu820, Leu694, Val702, Thr766	ND
54.	3,4-Dihydroxyfluorene	−7.8	Asp831, Glu738, Leu820, Val702, Ala719, Thr766, Thr830, Lys721	Lys721
55.	1,2-Dihydroxyfluorene	−7.7	Leu694, Leu820, Val702, Ala719, Thr830, Thr766, Asp831, Lys721	Asp831, Lys721
56.	Dehydrosafynol	−5.6	Phe699, Val702, Leu820, Ala719, Gly772, Asp831, Lys721, Met769	Met769
57.	Capillarin	−7.7	Leu764, Val702, Lys721, Met742, Thr766, Glu738, Thr830, Leu820, Met769, Asp831	Asp831
58.	2-Phenyl-3-(2-furyl) prop-2-enal	−6.2	Leu820, Asp831, Val702, Thr830, Lys721, Thr766, Ala719, Met769	Met769
59.	4 N-Acetyl-D-glucosamine	−5.4	Lys721, Thr830, Asp831, Gln767, Leu820, Met769, Ala719, Leu764, Met742, Thr766	Thr766
60.	2-Phenyl-3-(2-furyl) prop-2-enal!!	−5.1	Leu820, Ala719, Asp831, Met742, Thr830, Thr766, Val702, Lys721, Glu738	Lys721, Glu738
61.	Porphobilinogen	−6.1	Gly772, Leu768, Leu820, Val702, Ala719, Asp831, Lys721, Met769, Thr766, Thr830	Asp831, Lys721, Met769, Thr766, Thr830
62.	Carbidopa	−6.7	Ala719, Leu768, Leu820, Val702, Lys721, Asp831, Thr830, Met742, Thr766, Gln767, Met769	Thr766, Gln767, Met769

(Contd...)

Supplementary Table 1b: *(Continued)*

S. No.	Compound name	Binding energy (Kcal/mol)	Binding residues	Hydrogen bonding residues
63.	2-(2,4-Hexadiynylidene)-1,6-dioxaspiro[4.4]non-3-ene	−5.6	Gly772, Leu694, Thr766, Lys721, Leu764, Thr830, Met742, Ala719, Met769, Pro770	ND
64.	D-Erythro-Biopterin	−7	Thr830, Asp831, Leu694, Val702, Gly772, Ala719, Leu820, Leu768, Thr766, Glu738	Glu738
65.	Orinapterin	−6.5	Leu694, Leu820, Asp831, Lys721, Glu738, Val702, Thr766, Ala719, Met769, Thr830	Thr830
66.	Dyspropterin	−6.7	Leu764, Met742, Thr766, Ala719, Val702, Leu820, Asp831, Lys721	Lys721
67.	Primapterin	−6.7	Lys721, Ala719, Val702, Thr766, Met742, Thr830, Asp831, Leu820, Leu764	Leu764
68.	Sepiapterin	−6.3	Arg817, Val702, Thr830, Ala719, Leu764, Thr766, Glu738, Met742, Leu820, Asp831	Asp831
69.	N-Acetyl-D-glucosamine	−4.6	Leu764, Thr766, Trp393, Gly390, Asp831, Leu820, Phe445, Glu353, Pro325	Glu323, Trp393
70.	Glycolyl-D-mannosamine	−5.5	Leu723, Phe699, Gly833, Leu834, Asp831, Lys721, Glu738	Asp831, Lys721, Glu738
71.	Deoxyeritadenine	−6.5	Ala719, Gln767, Val702, Met742, Thr830, Leu820, Thr766, Asp831, Glu738, Lys721, Met760	Asp831, Glu738, Lys721, Met760
72.	2-(7'-Methylthio) heptylmalic acid	−5.7	Leu764, Met742, Thr830, Val702, Leu820, Ala719, Lys721, Asp831, Thr766	Lys721, Asp831, Thr766
73.	3-(7'-Methylthio) heptylmalic acid	−5.5	Leu764, Met742, Thr766, Ala719, Val702, Leu820, Leu694, Lys721, Glu738, Asp831, Thr830	Lys721, Glu738, Asp831, Thr830
74.	Purpuritenin B	−7.5	Met769, Ala719, Val702, Phe699, Lys721, Asp831, Cys773, Gly772, Leu820	ND
75.	Purpuritenin A	−7.2	Leu820, Gly695, Leu694, Thr830, Arg831, Thr766, Met742, Leu764, Lys721, Val702, Phe699	ND
76.	Coumatetralyl	−4.8	Leu694, Thr766, Thr830, Arg831, Met769, Gly772, Pro770	Lys720
77.	N-gamma-Glutamyl-S-propylcysteine	−5.4	Phe699, Leu820, Thr830, Leu764, Glu738, Met742, Thr766, Val702, Lys721, Asp831	Lys721, Asp831
78.	(all-E)-1,7-bis (4-hydroxyphenyl)-1,4,6-heptatrien-3-one	−7.4	Met742, Asp831, Thr830, Lys721, Leu820, Val702, Leu768, Leu694, Met769, Gly772, Thr766, Pro770	Thr766, Pro770
79.	(2S,4S)-Monatin	−7.7	Met742, Leu764, Ile765, Thr766, Met769, Leu820, Asp831, Ala719, Lys721, Thr830	Lys721, Thr830

Supplementary Table 2a: Docking results of phytoconstituents obtained from GC–MS characterization of EEPPR docked with ERα receptor.

S. No.	Compound name	Binding energy (Kcal/mol)	Binding residues	Hydrogen bonding residues
1.	1,1-Dimethoxypropane	−3.9	Lys449, Glu353, Gly390, Leu387, Met357, Ile386, Trp360, Pro324	ND
2.	3-(2-Methoxyethoxymethoxy)-2-methylpentan-1-ol	−4.1	Leu536, Trp383, Met522, Leu525, Glu523, Tyr526	ND
3.	1,3-Diethoxy-2-propanol	−4.3	Glu353, Met357, Pro324, Ile386, Trp360, Glu323, Lys449, Gly390, Pro325	ND
4.	2-(1-Ethoxyethoxy)-2-(2-oxiranyl) ethanol	−4.4	Glu353, Leu346, Leu349, Ala350, Leu384, Leu525, Leu391, Leu387	Glu353, Leu346
5.	Diethoxymethane	−3.3	Met357, Trp360, Leu387, Ile386, Pro325, Arg394, Glu353, Pro324, Lys449	ND
6.	1,1,3-Triethoxypropane	−4.2	Arg394, Leu387, Leu391, Leu384, Leu525, Phe404, Met421, Met388	ND

(Contd...)

Supplementary Table 2a: *(Continued)*

S. No.	Compound name	Binding energy (Kcal/mol)	Binding residues	Hydrogen bonding residues
7.	1,1,3-triethoxybutane	−4.6	Leu387, Met388, Ile424, Met421, His524, Gly521, Gly420, Leu384, Leu525, Met343, Leu346	ND
8.	D-allose	−5.0	Glu353, Ile386, Lys449, Leu387, Gly390, Arg394, Pro325, Pro324, Met357	Glu353, Ile386, Lys449, Pro325
9.	Methyl palmitate	−5.2	Leu391, leu387, Gku353, Ala350, Leu525, Thr347, Leu346	ND
10.	Palmitic acid	−5.6	Leu349, Leu391, Leu387, Met421, Leu384, Ile424, Gly420, Gly521, His524, Met343, Leu346, Leu525, Glu353, Ala350, Met388	ND
11.	Ethyl palmitate	−5.5	Leu391, Phe404, Met388, Trp383, Leu384, Leu525, Gly521, Gly420, Met343, Ile424, Met421, Leu346, Ala350, Leu349, Glu353, Leu387	ND
12.	Trimethylsilyl palmitate	−5.6	Leu354, Leu536, Trp383, Asp351, Ala350, Leu384, Phe404, Met421, Leu346, Met343, Leu525	ND
13.	Methyl linoleate	−6.0	Asp351, Thr347, Leu525, Leu391, Leu387, Ile427, Met388, Leu384, Leu349, Leu346, Phe404, Glu353, Trp383, Ala350	ND
14.	3,6-Octadecadienoic acid, methyl ester	−5.4	Tyr526, Thr347, Trp383, His524, Leu384, Met343, Ile424, Gly521, Ala350, Met388, Met522, Leu525	ND
15.	Linoleic acid	−5.0	Leu536, Val533, Pro535, Val534, Trp383, Met522, Leu525, Tyr526	Val534
16.	(R)-(-)-14-Methyl-8-hexadecyn-1-ol	−6.0	Leu384, Leu525, Leu391, Met421, Ile424, Phe404, Leu387, Met388, Glu353, Leu346, Leu349, Ala350	Glu353, Leu346
17.	trans, trans-9,12-Octadecadienoic acid, propyl ester	NA	Conformer generation is disallowed since too flexible	NA
18.	Dichloroacetic acid, tridec-2-ynyl ester	−6.1	Met421, Phe404, Ile424, Leu387, Leu391, Leu384, Gly521, Met388, Met421, Met343, Leu525, Ala350, Leu349, Leu346	ND
19.	Ethyl stearate	−5.4	Leu346, Leu387, Phe404, Asp351, Leu536, Trp383, Ala350, Leu525	ND
20.	Trimethylsilyl (9Z,12Z)-9,12-octadecadienoate	−6.2	Leu536, Ala350, Leu525, Met388, Leu384, Gly521, Leu346, Phe404, Leu387, Trp383, Met522,	ND
21.	Trimethylsilyl (5Z,8Z,11Z)-5,8,11-icosatrienoate	−6.3	Leu391, Phe404, Met388, Met422, Leu525, Trp383, Met522, Tyr526, Thr347, Glu353, Ala350, Leu346, Leu387, Leu384	ND
22.	Stearoxytrimethylsilane	−5.8	Leu391, Ala350, Phe404, Glu353, Leu346, Met343, Thr347, Trp383, Met528, Leu536, Met522, Leu525, Met388, Leu384, Ile424	ND
23.	2-Oxiranylmethyl palmitate	−5.7	Trp383, Thr347, Ala350, Leu525, Met528, Gly521, His524, Met421, Gly420, Ile424, Phe404, Leu384, Leu391, Leu346, Met388, Leu387	ND
24.	Trimethylsilyl (5Z,8Z)-7,7-dimethyl-5,8-icosadienoate	−6.3	Met421, Leu346, Leu384, Asp351, Leu354, Ala350, Trp383, Met522 Tyr526, Lys529, Leu525, Leu536, Thr347, Phe404	ND
25.	Trimethylsilyl tetracosanoate	−6.0	Met388, Phe404, Thr347, Leu346, Leu384, Leu391, Ala350, Trp383, Asp351, Lys529, Tyr526, Leu525, Leu536, Met421, Gly521, His524	ND
26.	Stigmasta-4,7,22-trien-3-α-ol			
27.	7β-Dehydrodiosgenin	NA	Conformer generation is disallowed since too many undefined stereo centers	NA
28.	Stigmast-5-en-3-ol	−7.4	Leu387, Met343, Trp383, Leu384, Leu525, Met522, Tyr526, Pro535, Val534, Val533, Leu536, Asp351, Thr347, Ala350	ND

(Contd...)

Supplementary Table 2a: *(Continued)*

S. No.	Compound name	Binding energy (Kcal/mol)	Binding residues	Hydrogen bonding residues
29.	Stigmast-5-en-3-yl (9Z)-9-octadecenoate	−7.4	Leu387, Met343, Trp383, Leu384, Leu525, Met522, Tyr526, Pro535, Val534, Val533, Leu536, Asp351, Thr347, Ala350	ND
30.	Trimethyl (octacosyloxy) silane	−6.2	Gly521, Met388, Leu391, Met343, Leu387, Leu346, Ala350, Thr347, Glu353, Trp383, Leu536, Tyr526, leu525, Leu384, His524, Gly420	ND
31.	3β -Acetoxystigmasta-4,6,22-triene	−8.6	Glu523, Tyr526, Leu536, Asp351, Leu539, Trp383, Leu525, Met522	ND
32.	Silane, trimethyl (stigmasta-5,22-dien-3beta-yloxy)	−8.8	Leu384, Ala350, Met343, Leu525, Met528, Lys529, Leu536, Trp383, Leu387, Asp351	ND
33.	Diosgenin	−10.1	Met522, Tyr526, Leu539, Leu536, Asp351, Trp383	ND
34.	Stigmast-5-ene, 3 beta-(trimethylsiloxy), (24S)	−8.5	Met522, Glu523, Leu525, Lys529, Val533, Val534, Leu539, Leu536, Tyr526	ND
35.	7-Ketodiosgenin acetate	−10.4	Val533, Lys531, Pro535, Leu536, Asp351, Trp383, Leu525, Leu346, Met343, Thr347, Met528, Lys529, Cys530	ND
36.	7 β-hydroxydiosgenin	NA	Conformer generation is disallowed since too many undefined stereo centers	NA
37.	Pennogenin	−9.1	Met522, Tyr526, Leu536, Val534, Asp351, Leu539, Trp383	ND

Supplementary Table 2b: Docking results of phytoconstituents obtained from LC–MS characterization of EEPPR docked with ERα receptor.

S. No.	Compound name	Binding energy (Kcal/mol)	Binding residues	Hydrogen bonding residues
1.	2,5-Dimethoxycinnamic acid	−5	Gly366, Leu306, Leu310, Gln314, Ala318, Arg363, Ala307, Lys362, Val364, Pro365, Asp369	Gly366
2.	3,4-Dimethoxycinnamic acid	−5.2	Glu423, Met421, Ile424, Val422, Ser527, His524, Glu523, Gly420, Lys520	Glu423, Ser527, Gly420
3.	2-Benzylsuccinic acid	−5	Val364, Asp369, Gly366, Ala307, Leu310, Leu306, Ala318, Pro365, Val368, Arg363	Val364, Asp369, Gly366
4.	Sinapyl aldehyde	−4.3	Gly390, Ile386, His356, Pro324, Met357, Glu353	ND
5.	6-Methoxymellein	−5.3	Leu525, Met522, Tyr526	Met522
6.	2-Benzylsuccinate	−5.7	Met421, Ile424, Leu387, Ala350, Leu391, Phe404, Glu353, Leu346, Leu525, Met343	ND
7.	4-Methyl-4-aza-5-pregnene-3,20-dione	−4.6	Asp480, Thr483, Leu479, Leu508, Leu511, Asn455, Ile451	Asp480, Thr483, Leu479
8.	Furapiole	−5.1	Leu525, Met522, Tyr526, Glu380, leu536, Trp383	ND
9.	1-(2-Methoxy-3,4-methylenedioxyphenyl)-1-propanone	−5.2	Gly521, Leu384, Met388, Leu391, Arg394, Phe404, Ala350, Leu387, Leu346, Leu525	ND
10.	4-Methyl-4-aza-5-pregnene-3,20-dione	−7.0	Pro365, Gly366, Val368, Ala307, Leu310, Gln314, Ser317, Asp 321, Ala318, Arg363, Lys362, Val364	Gly266
11.	Butanedioic acid	−6.0	Ala307, Pro365, Val368, Leu310, Gln314, Ser317, Asp 321	ND
12.	Gallic acid	−4.0	Ala318, Arg363, Phe461, Leu462, Lys467, Asp374, Thr371	Tyr525
13.	Chlorogenic acid	−4.8	His373, Ser468, Phe461, Leu462, Lys467, Asp374, Thr371	Met357
14.	Sumatriptan	−5.6	Glu523, Asn519, Lys529, leu525, Tyr525, Met522	ND
15.	4-(8, 9-Dihydro-8-methyl-7H-1, 3-dioxolo (4,5-H) (2,3) benzodiazepin-5-yl) benzenamine	−4.9	Glu523, Asn519, Leu820, Val702, Met357, Glu353	Gly390
16.	Tetrahydrothiophene-2-carboxylic acid	−4	His373, Sre468, Phe461, Leu462, Lys467, Asp374, Thr371	ND
17.	3-methyl sulfolene	−4.3	Gly390, Ile386, His356, Pro324, Met357, Glu353	Leu320

(Contd...)

Supplementary Table 2b: *(Continued)*

S. No.	Compound name	Binding energy (Kcal/mol)	Binding residues	Hydrogen bonding residues
18.	3-Oxo-3-ureidopropanoate	−5	Met357, Leu387, Pro324, Lys449, Gly390, Arg394, Glu353, Ile386	Glu353
19.	5-N-Methyloxaluric acid	−4.5	Arg503, Leu495, Leu489, Glu444, Gln441, Glu443, Ala493	ND
20.	3-Hydroxy-3-methyl-glutaric acid	−4.2	Leu308, Ala312, Asp484, Thr485, Lys481, Leu310	Asp484, Thr485, Lys481, Leu310
21.	Levoglucosan	−4.6	Ser488, Thr465, Leu462, His373, Asp374, Thr371, Lys467	Thr465, His373, Asp374, Thr371
22.	2-Hydroxyadipic acid	−4.3	Pro324, Gly390, Glu323, Ile386, Lys449, Glu353, Pro325	Glu323
23.	3,3-diethoxy-1-propanol	−4.9	Leu386, Ile386, Arg394, Gly390, Glu323, Pro324, Pro325, Glu353, Lys449, His356, Met357	Glu323, Pro324, Glu353,
24.	2S-Hydroxy-hexanedioic acid	−3.7	Ala430, Ile510, His513, Thr431, Arg434	His513
25.	3-Hydroxymethyl-glutaric acid	−4.5	Leu387, Ile386, Lys449, Glu353, Phe445, Gly390, Pro324, Arg394, Met357	Ile386
26.	L-Rhamnono-1,4-lactone	−4.7	Ile386, Gly390, Arg394, Ile326, Pro325, Leu387, Pro324, Glu353, Met	Ile386
27.	2-Dehydro-3-deoxy-L-rhamnonate	−3.9	His373, Ser468, Lys467, Thr371, Asp374, Glu471	His373, Thr371
28.	2-Dehydro-3-deoxy-D-fuconate	−4	Thr485, Lys481, Asp484, Ala312, Leu310, Thr311, Met315	Thr485, Lys481
29.	(R)-2-Ethylmalate	−3.8	Ile510, Thr431, Ala430, Arg434, His513	ND
30.	5-Ureido-4-imidazole carboxylate	−5.4	Ser463, Phe461, Ser468, His373, Asp374, Lys467, Leu462, Thr465	Ser463 Ser468
31.	Magnesium propionate	−1.6	Ser432, Leu429, Ser433, Arg436	ND
32.	1-Naphthoic acid	−6	Arg434, Thr431, Ala430, His513, Ile510	Ala430
33.	Menadoine	−5.6	Arg434, Ala430, Thr431, Ile510, His513	ND
34.	Dehydromatricaria ester	−4.1	Met522, Leu525, Tyr526	ND
35.	Methyl (Z)-dec-2-en-4,6,8-triynoate	−4.2	Leu820, Ala719, Leu764, Met742, Asp831, Val702, Leu694, Glu738	Leu820
36.	1-Hydroxy-2-naphthaldehyde	−6.4	Leu346, Phe404, Ile424, Gly521, Leu384, Leu525, Ala350	ND
37.	2-Naphthoic acid	−6.7	Ala430, Ile510, His513, Gln506, Leu509, Arg434, Thr431	ND
38.	3Z-Undecene-5,7,10-triynoic acid	−4.2	Gln541, Leu489, Val316, Ser317, Asp313, Glu443, Glu444	Asp313
39.	4E-Undecene-6,8,10-triynoic acid	−5.1	Ile368, Gly390, Lys449, Met357, Pro324, Leu387, Glue353, His356, Glu323, Ile326	ND
40.	L-Ascorbic acid	−4.7	Val422, Glu423, Ile424, Met421, Gly423, Lys520, Glu523, His524	Glu423, Gly423
41.	2-Ketogulonolactone	−4.5	Ala348, Lys481, His488, Met315, Thr863, Thr485, Asp484	Lys420
42.	Glucuronolactone	−4.3	Leu310, Lys481, His488, Ala312, Met315, Thr311, Thr485, Asp484	Ala312
43.	5-Dehydro-4-deoxy-D-glucuronate	−3.9	Leu370, Glu470, Glu471, Lys467, Thr371, his474, Asp369	Glu471, Asp369
44.	(4S)-4,6-Dihydroxy-2,5-dioxohexanoate	−4.4	Trp393, Ile326, Gly390, Pro324, Glu353, Lys449, Phe445, Glu323	Lys449, Glu323
45.	2-Hydroxy-3-oxoadipate	−3.9	Ile451, Thr483, Leu508, Asp480, His476, Leu479	Thr483, Asp480, His476, Leu479
46.	2-Hydroxydibenzofuran	−7.3	Leu525, Leu346, Leu391, Phe404, Leu387, Glu353, Ala350, Leu384	ND
47.	Dibenzo-p-dioxin	−7.7	Met357, Ile386, Gly390, Lys449, Ile326, Phe445, Trp393, Arg394, Glu353, Pro324	Lys449
48.	4-Hydroxy-4-methyl-2-oxoglutaric acid	−4.6	Pro325, Ile326, Gly390, Lys449, Phe445, Arg394, Glu353, Pro324, Glu323	Pro324, Glu323

(Contd...)

Supplementary Table 2b: *(Continued)*

S. No.	Compound name	Binding energy (Kcal/mol)	Binding residues	Hydrogen bonding residues
49.	D-Glucurono-6,2-lactone	−4.5	Ser463, Ser468, leu462, Lys467, His373, Asp374, Thr371, Thr465	Lys467, His373, Asp374, Thr371, Thr465
50.	(4S,5S)-4,5-Dihydroxy-2,6-dioxohexanoate	−4.6	Ile386, Lys449, Pro324, Ile326, Arg349, Glu353, Gly390, Met357	Ile386, Glu353
51.	D-Galacturonolactone	−4.2	Leu462, Ser463, Ser468, Thr465, Lys467, Thr371, His373, Asp374	Ser463, Thr371, His373, Asp374
52.	4-Hydroxybenzophenone	−5.9	Ala430, Arg434, His513, Ile510, Thr431, Ser433	Ser433
53.	Splitomicin	−7.8	Gly521, Met434, Leu436, Phe404, Ala350, Leu384, Leu525, Met421	ND
54.	3,4-Dihydroxyfluorene	−7.3	Ile424, Leu346, Met421, Phe404, Glu353, Ala350, Leu387, Leu384, Leu525	ND
55.	1,2-Dihydroxyfluorene	−7.5	Gly390, Lys449, Leu387, Ile386, Met357, Pro324, Gle353, Pro325, Phe445, Ile326, Trp393	ND
56.	Dehydrosafynol	−5.2	His513, Arg434, Gln506, Gln502, Ala505, Leu509, Ile510, Thr431	Thr431
57.	Capillarin	−5.7	Met522, Glu523, Asn519, Tyr526, Leu525	ND
58.	2-Phenyl-3-(2-furyl) prop-2-enal	−5.3	Ala430, Arg434, Thr431, Ile510, His513	ND
59.	4 N-Acetyl-D-glucosamine	−5.9	Arg394, Leu387, Phe445, ile386, Trp393, Glu327, Pro325, pro324, Gly390, Lys449, Glu353	Arg394
60.	2-Phenyl-3-(2-furyl) prop-2-enal!!	−6.5	Met522, Glu523, Tyr526	ND
61.	Porphobilinogen	−4.3	His513, Leu509, Ile510, Arg434	ND
62.	Carbidopa	−5.1	Arg477, Asp473, Glue471, Asp369, Glu470, His474	Arg477, Asp473, Glue471, Asp369
63.	2-(2,4-Hexadiynylidene)-1,6-dioxaspiro[4.4]non-3-ene	−6.3	Ala312, Asp484, Arg394, Leu387, Phe445, Trp393, Glu327, Pro325, Gly390, Lys449, Glu353	Leu420
64.	D-Erythro-Biopterin	−5.2	Ala312, Asp484, Leu310, Lys481, Arg477, Asp480, Leu308, Thr311	ND
65.	Orinapterin	−5.5	Ala318, Pro365, Ala307, Asp369, Val368, Gly366, Arg363,	Ala307, Asp369, Gly366
66.	Dyspropterin	−5.2	Ile510, His513, Arg434, Thr431, Ala430	Ala430
67.	Primapterin	−5.6	His513, Thr431, Arg434, Ser433, Ala430, Ile510	Ser433
68.	Sepiapterin	−4.7	Ala430, Ile510, Leu509, Ile510, His513, Ala369	ND
69.	N-Acetyl-D-glucosamine	−4.2	Glu323, Pro324, Trp393, Gly390, Ile326, Arg394, Phe445, Glu353, Pro325	Glu323, Pro324, Trp393
70.	Glycolyl-D-mannosamine	−4.9	Arg394, Glu323, Phe445, Pro324, Ile386, Gly390, trp360, Lys449, Met357, Glu353, Leu387, Pro325, Ile326	Lys449, Glu353
71.	Deoxyeritadenine	−5.5	Ile510, Arg343, Met347, Ser433, Ala430, Thr431, His513	Ser433
72.	2-(7'-Methylthio) heptylmalic acid	−4.4	Ale312, Leu310, Asp484, Lys481, Asp480, Arg477, Leu308, Thr485, Thr311	Thr485
73.	3-(7'-Methylthio) heptylmalic acid	−5.2	Ile386, Gly390, Lys449, Phe445, Trp393, Glu323, Ile326, Pro325, pro324, Glu353, Leu387	Pro325, pro324, Glu353
74.	Purpuritenin B	−6.9	Met522, Tyr526, Leu525, Glu523	ND
75.	Purpuritenin A	−5.2	Pro535, Tyr526, Met522, Leu536	Leu536
76.	Coumatetralyl	−4.5	Leu694, Thr523, Thr630, Arg431, Met769, Gly772, Pro770	ND
77.	N-gamma-Glutamyl-S-propylcysteine	−4.9	Glu523, Tyr526, Lleu525, Met522, Leu536, Trp383	Glu523, Met522
78.	(all-E)-1,7-bis (4-hydroxyphenyl)-1,4,6-heptatrien-3-one	−5.9	Thr431, Arg434, Ser433, Arg412, Leu429, Ala430, Ile510, His513	ND
79.	(2S,4S)-Monatin	−5.9	Leu346, Met421, Met343, Gly420, Glu419, Gly521, Thr347, Leu525, Asp351, Trp383, Ala350, Phe404, Glu353, Arg394, Leu428, Leu387	Arg394